San Jose State University
SJSU ScholarWorks

Master's Theses | Master's Theses and Graduate Research

Summer 2016

Effects of Zoledronate During Simulated Weightlessness on Bone Structure and Mechanics

Ryan T. Scott
San Jose State University

Follow this and additional works at: https://scholarworks.sjsu.edu/etd_theses

Recommended Citation

Scott, Ryan T., "Effects of Zoledronate During Simulated Weightlessness on Bone Structure and Mechanics" (2016). *Master's Theses*. 4738.
DOI: https://doi.org/10.31979/etd.s375-rchn
https://scholarworks.sjsu.edu/etd_theses/4738

This Thesis is brought to you for free and open access by the Master's Theses and Graduate Research at SJSU ScholarWorks. It has been accepted for inclusion in Master's Theses by an authorized administrator of SJSU ScholarWorks. For more information, please contact scholarworks@sjsu.edu.

EFFECTS OF ZOLEDRONATE DURING SIMULATED WEIGHTLESSNESS ON BONE STRUCTURE AND MECHANICS

A Thesis

Presented to

The Faculty of the Department of Kinesiology

San José State University

In Partial Fulfillment

of the Requirements for the Degree

Master of Arts

by

Ryan T. Scott

August 2016

© 2016

Ryan T. Scott

ALL RIGHTS RESERVED

The Designated Thesis Committee Approves the Thesis Titled

EFFECTS OF ZOLEDRONATE DURING SIMULATED WEIGHTLESSNESS ON BONE STRUCTURE AND MECHANICS

by

Ryan T. Scott

APPROVED FOR THE DEPARTMENT OF KINESIOLOGY

SAN JOSÉ STATE UNIVERSITY

August 2016

Dr. Peggy Plato	Department of Kinesiology
Dr. Shelley Cargill	Department of Biology
Dr. Joshua Alwood	NASA Ames Research Center

ABSTRACT

EFFECTS OF ZOLEDRONATE DURING SIMULATED WEIGHTLESSNESS ON BONE STRUCTURE AND MECHANICS

by Ryan T. Scott

Spaceflight causes astronauts to experience an unbalanced level of bone remodeling favoring resorption. The combination of an antiresorptive drug and weightlessness may have negative effects on the mechanical and structural properties of bone by increasing elastic stiffness but diminishing plasticity. At 16 weeks of age, skeletally postpubescent male mice (*n* = 32, C57BL/6) were evenly divided and subcutaneously given either zoledronate (45 μg/kg) or vehicle (saline, same volume). Three days postinjection, half of each group were divided to undergo 3 weeks of hindlimb unloading or act as a control undergoing normal ambulation (*n* = 8 for each of the 4 groups). Ex vivo μCT assays showed zoledronate preserving cancellous mineral, bone, and cortical bone. Hindlimb unloading reduced cortical bone. Three-point bending of the femoral mid-shaft showed zoledronate increased stiffness, ultimate force, and total energy (+28%, +17%, +15%, respectively). Hindlimb unloading reduced stiffness but increased postyield displacement, a measurement of plasticity (-29%, +20%, respectively). The combined treatment resulted in increased stiffness, with zoledronate not modulating the hindlimb unloading main effect on postyield displacement. Though stiffness increased, contrary to the hypothesis, the combination of zoledronate and hindlimb unloading did not result in a decreased plasticity.

ACKNOWLEDGEMENTS

First, I would like to thank my parents. I am also sincerely grateful to Dr. Joshua Alwood for the opportunity to work with him at the NASA Ames Research Center's Bone and Signaling Laboratory, and for providing the samples. I would also like to thank all of the NASA Ames Bone and Signal Laboratory colleagues who assisted in this study. In particular, I greatly appreciated the scientific discussions and support from all my colleagues of the Alwood team: Mohit Nalavadi, Megan Pendleton, Nicholas Thomas, Catherine Choi, and Rebecca Stevick. I am grateful for NASA's Space Biology New Investigator Award (NNH12ZTT001N) for supporting this work.

In addition, I would like to thank several other researchers in the Bone and Signaling Laboratory: Dr. Ruth K. Globus, Dr. Eduardo Almeida, Dr. Elizabeth A. Blaber, Dr. Ann-Sofie Schreurs, Dr. Yasaman Shirazi-Fard, and Dr. Candice T. Tahimic. Also at NASA Ames, I greatly appreciate the inspiration from Dr. Jacob Cohen.

I would like to convey my deepest thanks to Dr. Peggy Plato, my thesis advisor from the SJSU Kinesiology Department. I would also like to thank Dr. Shelley Cargill, Dr. Joanne Kerr, Dr. Daniel Holley, and Dr. Shannon Bros, all from the SJSU Biology Department. Each played a wonderful role in my experience at SJSU, as well as providing assistance in this project. I am additionally grateful to be a California State University 2015-2016 Sally Casanova Pre-Doctoral Scholar, which provided support for this work.

Table of Contents

List of Tables

List of Figures

Chapter I

Introduction

Problem

A central challenge in conducting human spaceflight missions is the maintenance of bone health. More basic scientific research is needed to elucidate the deleterious effects of microgravity on animal and human bones. In the coming decades, missions will be scheduled to advance humanity into a new frontier of exploration past the Van Allen belts, toward Mars, establishing lunar bases, or toward Lagrange points. A better understanding of bone mechanobiology will be needed to facilitate the development of effective countermeasures and mitigation regimens to enable long-term human spaceflight.

Frost (2003) is credited with first describing the skeletal system's biological interaction with its environment being akin to a "mechanostat," with the bone structure adapting to the specific imposed environmental demands. This bone remodeling is accomplished through both bone formation and resorption. Other factors in this mechanostat theory include bone geometry, metabolic status, genotype, tissue interaction, and local tissue response (Beaupre, Orr, & Carter, 1990). Osteoclasts are the cells of the bone responsible for resorption, osteoblasts are responsible for bone formation, and osteocytes are thought to coordinate the response to mechanical and metabolic signals (Crockett, Rogers, Coxon, Hocking & Helfrich, 2011).

Adverse spaceflight-related bone alterations are partly due to prolonged periods of weightless unloading referred to as microgravity. This arises from a lack of muscular and gravitational forces upon bone as would be experienced on Earth. The lack of weight experienced by astronauts assigned to the International Space Station (ISS) is from free fall. The vacuum of space (outside of Earth's atmosphere) and the gravity of Earth both factor into objects falling toward Earth at the same rate, irrespective of an object's mass (Turner, 2000). This unloading effect from microgravity on the musculoskeletal system negatively alters bone structure, reduces the collagen matrix mineralization, impacts osteocellular activity, decreases the amount of bone, and impairs mechanical properties (Keyak, Koyama, LeBlanc, Lu, & Lang, 2009; Smith et al., 2014). This can lead to increased probability of fracture. For astronauts who are tasked with physically strenuous work such as extravehicular activities, this could lead to devastating consequences during spaceflight missions (Orwoll et al., 2013).

During 6-month ISS missions, bone remodeling favors resorption by osteoclasts (Smith, Wastney, et al., 2005). This increase in bone resorption is notable, with bone formation undergoing little change compared to ground controls (Calliot-Augusseau et al., 1998; Smith, Zwart, Block, Rice, & Davis-Street, 2005). Astronauts present with a rate of bone loss about 10 times greater than the rate of bone loss by postmenopausal women on earth (Smith et al., 2014).

Microgravity-induced bone loss occurs preferentially at the site of weight-bearing bones, with an early and pronounced loss of cancellous bone (Collet et al., 1997; Lang et al., 2004; LeBlanc et al., 2000; Vico et al., 2000). Vico and colleagues (2000) investigated astronauts who served on 2-month and 6-month missions. The loss of vertebral bone mineral density (BMD) was 0.9% per month, and hip BMD losses were 1.4% per month. Through the application of computed tomography scanning and finite element modeling techniques, the loss of bone strength in the femur of astronauts has been shown to be much greater than the changes in BMD (Keyak et al., 2009).

With the recent ISS utilization of the Advanced Resistive Exercise Device (ARED), crews have had access to high-force resistance training protocols. The ARED is able to generate absolute loads up to 272 kg (600 lbs) of force (Loehr et al., 2010). This has resulted in bone formation increases during flight (Smith et al., 2014). While the inclusion of ARED was the first successful countermeasure for astronaut bone loss by increasing bone formation, this has not necessarily solved the challenge of heightened bone resorption. Spaceflight ARED heavy resistance training did not inhibit the increases of osteoclast activity and bone resorption. Both bone resorption and bone formation indices from blood and urinary markers have been shown to stay above prelaunch baselines during missions with astronauts using ARED (Smith et al., 2012). The increase in the skeletal remodeling rate is referred to as high bone turnover, with increases in both osteoblast bone formation and osteoclast bone resorption. Chronic high

bone turnover experienced by astronauts during long duration spaceflight raises potential concerns of negative structural and mechanical side effects on bone health, such as atypical femoral fractures and stress fractures. Additional countermeasures to specifically inhibit bone resorption have been researched and considered for astronauts during extended space missions (LeBlanc et al., 2013).

Zoledronate, a member of the bisphosphonate class of drugs, has been proposed for long-term spaceflight missions as an antiresorptive countermeasure targeting osteoclasts. It can prevent weightlessness-induced bone loss in a hindlimb unloading rodent model, and it is currently prescribed by physicians as an effective agent for the management of osteoporosis (Lloyd, Travis, Lu, & Bateman, 2008; Reid et al., 2002).

Medicinal chemists specifically developed zoledronate, which contains a nitrogen atom within heterocyclic rings at the R^2 side chain of the carbon atom of the phosphate-carbon-phosphate (P-C-P) backbone common among all bisphosphonates (Kavanagh et al., 2006; Russell, 2011). Zoledronate is the most potent antiresorptive drug, having the highest mineral binding affinity (Ebetino et al., 2011). With bisphosphonates inhibiting osteoclasts and bone resorption, the amount of hydroxyapatite (HAP) mineral increases due to unhindered osteoblast bone formation activity. The result is a greater amount of mineral per bone volume (Allen & Burr, 2007; Boivin, Chavassieux, Santora, Yates, & Meunier, 2000; Burr et al., 2003). Whole-bone mechanical properties of

stiffness and strength (ultimate force) increase with bisphosphonate treatments (Allen & Burr, 2007, 2011). Mineral HAP is considerably stiffer than the bone collagen molecules to which it is bound (Fratzl & Weinkamer, 2007).

Several factors affect the pharmacological impact and lasting potency of bisphosphonates. Once delivered through the bloodstream, the bisphosphonate compounds specifically target and bind to bone according to the drug's mineral binding affinity. Osteoclasts migrate and undergo a process of polarization, vesicular trafficking, mineral dissolution, and ultimately bone resorption. The bisphosphonate previously bound to the bony matrix is released as bone is resorbed and taken up into the cell (Coxon & Taylor, 2008).

Once taken up by the osteoclast, bisphosphonates inhibit bone resorption through intracellular effects. When a nitrogen-containing bisphosphonate is incorporated into the osteoclast cell, it has been shown to interrupt a prominent target enzyme in the mevalonate biosynthetic pathway: farnesyl pyrophosphate synthase (FPPS) (Amin et al., 1992). The interruption of this pathway leads to substrate depletion of farnesyl pyrophosphate (FPP) and geranylgeranyl pyrophospate (GGPP) lipid groups (Rogers et al., 2000). Small GTPase proteins including Rac, Rho, and Rabs each rely on posttranslational covalent addition (prenylation) of these lipid substrates onto their respective cysteines. This cysteine residue is located fourth from the end in a CaaX or CxC motif, adjacent to the polybasic region of the protein chain (Weivoda & Oursler, 2014; Zhang & Casey, 1996). Without prenylation of FPP and GGPP, the small GTPases do not

localize correctly in the cell membrane to exert their specific actions, relying on FPP and GGPP as anchors in the cell membrane (Zhang & Casey, 1996). Without properly functioning small GTPases, many functions of the osteoclast and resorption are impaired: vesicle transport, cellular polarization, actin reorganization, and overall cell activity (Coxon, Thompson, & Rogers, 2006; Crockett et al., 2011; Ory, Brazier, Pawlak, & Blangy, 2008; Rogers et al., 2000). Dunford and colleagues (2001) examined zoledronate in vivo and in vitro. They found that its antiresorptive potency stems from the nitrogen atom within the heterocyclic rings inhibiting FPPS rather than the degree of cellular uptake or pharmacokinetics of zoledronate. Two other pharmacodynamic factors of bisphosphonates include the critical inhibition of the dissolution of HAP mineral, and the different binding affinity profile of each bisphosphonate based on its chemical structure (Nancollas et al., 2006; Russell, 2011).

The great cost of conducting human and rodent science on the ISS has led researchers to pursue ground analogs to simulate conditions of microgravity-like weightlessness. One such protocol is the 30° hindlimb unloading (HU) model in mice and rats (Morey-Holton & Globus, 2002). Musculoskeletal disuse simulates weightlessness, which increases osteoclast activity and decreases bone structure (Heer, Baecker, Mika, Boese, & Gerzer, 2005; Nabavi, Khandani, Camirand, & Harrison, 2011; Tamma et al., 2009). Animal studies allow techniques of both destructive mechanical testing and radiographic structural morphology scanning. These studies also have scientific value in enabling

researchers to control study variables such as duration, unloading, age, drug administration, and temperature.

Lloyd et al. (2008) provided evidence that, in a growing mouse model (6 weeks old), an effective antiresorptive dosage of zoledronate is 45 μg/kg to counteract skeletal hindlimb unloading and to maintain bone stiffness. Pozzi and colleagues (2009) examined zoledronate's efficacy on bone remodeling in the growing mouse model (5 weeks old), reporting that 100 μg/kg was no more effective of an antiresorptive than 50 μg/kg. Utilizing a rat immobilization model with the right hindlimb affixed to the abdomen, Khajuria, Razdan, and Mahapatra (2015) found a zoledronate dosage of 50 μg/kg to be effective at countering the deleterious impact of limb immobilization on mechanical properties.

Potential negative side effects on the mechanical and structural properties of astronaut bone should be examined when heightened turnover, high-force exercise, and antiresorptive bisphosphonate drug treatments are combined. This is of note due to clinical concerns of atypical femoral fractures along the diaphysis and osteonecrosis of the jaw with long-term bisphosphonate use (Iwata, Mashiba, Hitora, Yamagami, & Yamamoto, 2014; Reid, 2009; Shane et al., 2010; van der Meulen & Boskey, 2012). Zoledronate is an attractive countermeasure candidate due to its intravenous 6-month injection timeline. Other bisphosphonates require a weekly oral dose and have several negative drawbacks such as possible gastrointestinal intolerability, myalgia, and arthralgia (LeBlanc et al., 2013; Silverman & Christiansen, 2012).

Work by Currey (2012) illustrated the principle that as the degree of mineralization increases in bone, there is a corresponding linear increase in stiffness. As a bone becomes more mineralized, it becomes stiffer, but at a certain point there is a rate of diminishing returns. Currey generated data that argued the elastic stiffness and plasticity of bone can have an inverse relationship. If a bone becomes too stiff from overmineralization, it becomes more brittle and less tough. Brittleness is an inverse measure of plasticity. Brittleness is also measurable in terms of reduced strain required to initiate permanent deformation, the point where bone structural integrity yields.

The organic bone matrix, with its major constituent of collagen, is disproportionately responsible for bone plasticity and contributes to toughness. Small changes to the quality of bone collagen would have little effect on bone stiffness, with mineral HAP having around 114 GPa (gigapascals) and collagen 1.5 GPa (Zioupos, Currey, & Hamer, 1999). Because collagen is composed of numerous organic constituents such as crosslinks and water, changes in collagen quality and composition could have dramatic effects on bone toughness and plasticity. From the yield point onwards, it is the collagen and the organic matrix that absorb and disperse energy until abject failure of the bone (Burr, 2002; Currey, 2012; Currey, Brear, & Zioupos,1996).

Zoledronate treatment results in greater bone mineralization and retention. The purpose of this study was to assess the effects of zoledronate on bone mechanical and structural properties of bone during simulated weightlessness. It

was hypothesized that the zoledronate-treated mice experiencing simulated weightlessness would increase their whole-bone elastic stiffness but have diminished mechanical plasticity, making the bones stiffer but more brittle.

Objective

The objective of this work was to examine the effect of zoledronate on bone mechanical and structural properties in an experimental model designed to mimic spaceflight weightlessness. The 30° hindlimb unloading model was used to mimic the effects of weightlessness and induce musculoskeletal disuse in mice. The expectation is that this work will add to the body of knowledge to enhance the development of countermeasures to enable prolonged space exploration in the future.

Delimitations

This study was focused on the mechanical and structural impact of hindlimb unloading musculoskeletal disuse and zoledronate administration in mice. Treatment effects were examined ex vivo using the left femur from the animals. All mice were of the same age (16 weeks), gender (male), genetic bred strain (C57BL/6), and they were subject to similar housing, feeding (ad libitum), and handling.

Limitations

This experimental model was designed to simulate the conditions astronauts experience in spaceflight. Although mice and humans are both mammalian species, there are a few significant differences. They include the

size of human versus mouse bone and the growth plate of bones. Unlike the human growth plate, which closes at maturity, the mouse growth plate does not fully attain closure at any point in the lifespan. Additionally, mouse cortical bone presents with lamellae and adjacent osteocytic lacunar networks rather than the osteonal Haversian canal networks found in human cortical bone. Lastly, the mechanical properties of toughness and plasticity of bone were measured in this study. There is consensus in the field that the behavior and characteristics of collagen are responsible for the plasticity of bone (Burr, 2002; Viguet-Carrin, Garnero, & Delmas, 2006). Without an assay for collagen measurements, a full characterization of the molecular changes due to the treatment is not possible.

Overview

This thesis is divided into five chapters. Chapter II presents background on general bone structure, the femurs of both humans and mice, the hindlimb unloading model, micro-computed tomography (μCT) scanning, and the 3-point (3-pt) bending mechanical test. Chapter III provides specifics on study design, specimen preparation, data collection procedures, and statistical analysis. Results are presented in Chapter IV, followed by Chapter V, which includes conclusions, a discussion of the significance of the findings, and recommendations for future work.

Chapter II

Review of Literature

Bone Components

The skeleton has a hierarchical level of organization. While there are variations between species in the shapes of their bones, all bones on the gross level are considered to be either long, short, flat, sutural, pneumatic, irregular, or sesamoid. When a long bone is examined, there is identification of distal and proximal epiphyses separated by the intervening diaphysis. In a femur, there is a distal region known as the metaphysis, which is rich with a lattice, strut-like plate network referred to as cancellous bone. This structure is extremely porous, with the thickness of individual trabeculae measuring 100 to 300 μm in humans (Fratzl & Weinkamer, 2007). Encapsulating the bone's cancellous compartment is a sturdy layer with low porosity, known as cortical bone.

Mice provide researchers a remarkable model to explore the biology of the mammalian skeleton and enable extensive studies of disease. The model is utilized to understand structural and mechanical properties of bone (Jepsen, Silva, Vashishth, Guo, & van der Meulen, 2015). Despite a big difference in lifespan (human ≈ 80 years, mouse ≈ 2 years), they both present with analogous age-related bone changes at similar points in their respective lifespans (Ferguson, Ayers, Bateman, & Simske, 2003; Halloran et al., 2002). A few aspects of the mouse model are of note. Mouse bones have different anatomical skeletal arrangements and ambulate in a quadrupedal manner. This translates

to a specific distribution of skeletal stresses and strains based upon ground reaction forces and muscles generating forces according to ambulatory patterns (Figure 1).

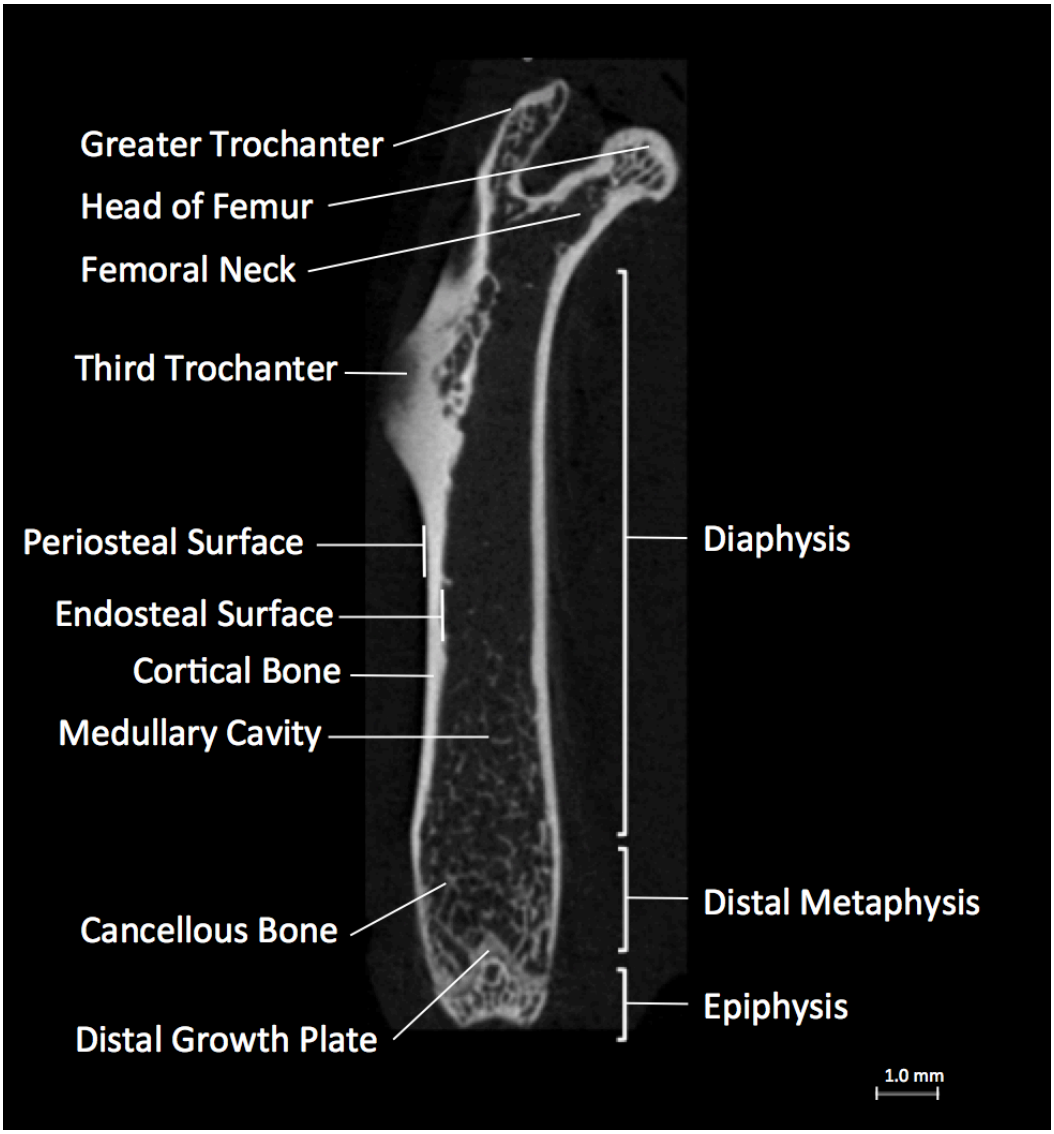

Figure 1. Mouse femoral anatomy. Internal view of a left mouse femur from a coronal plane slice at the third trochanter.

When examining the internal coronal plane view of a left mouse femur one sees the outermost radius is comprised of cortical bone, with a corresponding outermost connective tissue layer known as the periosteum. Spanning the length of the diaphysis is a central cavity known as the medullary cavity, which is lined with a bony connective tissue layer called the endosteum. Of note, mice present with a prominent third trochanter, which differs from that of normal human anatomy. The third trochanter of the mouse receives tendons from the hindlimb muscles, which then insert into the third trochanter's periosteal layer (Hamrick, McPherron, Lovejoy, & Hudson, 2000).

At the tissue level, there are spatial arrangements that differ between cortical bone and concentrated sections of individual trabeculae of cancellous bone. In different animals, various degrees of cortical organization are seen. This organizational network of bone can be classified as being either woven (more chaotic, irregular), lamellar (organized smoothly, parallel structure), or osteonal (concentric lamellar bone) (Wagermaier, Klaushofer, & Fratzl, 2015). Each organization depends upon the configuration of individual collagen molecules, mineralization, and the extrafibrillar matrix consisting of proteoglycans and noncollagenous proteins, which also impact the relative mechanical properties of each bony tissue (Doblaré, García, & Gómez, 2004).

Human cortical bone predominantly displays osteonal Haversian networks, with concentric lamellae (layers of bone matrix) wrapped around a central Haversian canal. Mouse bone is also characterized as lamellar bone but

not to the same magnitude of concentric organization. Lateral and medial to the lamellar mouse cortical bone, layers of fibers extend toward the endosteal and periosteal surfaces. Through three different microscopy techniques, Kerschnitzki and colleagues (2011) concluded that, in the femur of the mouse, this cortical endosteal and periosteal bone deposition pattern corresponds to an alignment of the osteocytic cytoplasmic processes and the structural arrangement of the collagen matrix. The differing pattern between mouse and human bone is an understood condition when drawing mechanobiological conclusions from scientific research.

There are three major bone cell types: osteoblasts, osteocytes, and osteoclasts. Osteoblasts are mononucleated cells derived from mesenchymal stem cells via the osteoprogenitor pathway (Blaber et al., 2014). They are critical in bone formation via an exocytotic release of Type I collagen as well as many noncollagenous bone proteins (Neve, Corrado, & Cantatore, 2011; Orriss, Burnstock, & Arnett, 2010). Before HAP minerals are deposited, the organic cartilaginous layer is referred to as an osteoid. At the conclusion of osteogenesis, levels of the osteoblast-dependent alkaline phosphatase mRNA decline drastically, followed by around 70% of mature osteoblasts undergoing apoptosis (Neve et al., 2011). Some of the osteoblasts become incorporated into the newly formed osteoid that they secreted and differentiate into osteocytes (Franz-Odendaal, Hall, & Witten, 2006; Manolagas, 2000).

Osteocytes are contained within protective cavities, referred to as lacunae and form an interconnected network of canalicular cytoplasmic projections within the bony matrix. These networks allow passageway of metabolites and are thought to mediate responses to mechanical loading. Cancellous tissue has a considerably higher porosity than cortical, with most cortical porosity accounted for by the lacunae, vessels, and nerves. Osteocytes comprise 90-95% of all bone cells (Bonewald, 2011).

Responsible for bone resorption, osteoclasts are usually multinucleated and develop into bone-specific macrophages from the hematopoietic cell lineage of differentiating monocyte/macrophage precursors (Boyle, Simonet, & Lacey, 2003). Functioning osteoclasts undergo a stepwise progression to create an acidic resorption lacunar pit atop the bony matrix. Osteoclasts first attach and begin cellular polarization, initiating the bone resorption process, followed by a cessation of bone resorption (Mellis, Itzstein, Helfrich, & Crockett, 2011). The polarization/attachment stage involves a rearrangement of the cell's cytoskeleton to form a "sealing zone" formed by adhesive podosomes on the bone matrix surface (Lakkakorpi & Väänänen, 1996; Luxenburg et al., 2007). Osteoclasts are motile cells that migrate over the bony matrix and rely on the ability of these podosomes to disassemble and assemble quickly (Luxenburg, Parsons, Addadi, & Geiger, 2006; Mellis et al., 2011).

The full breadth of molecular signals and energy pathway downregulatory mechanisms that result in podosome disassociation, a halt to cell motility, and

cessation of resorption at the lacunar pit are still being investigated (Mellis et al., 2011). There are several physiological regulators that influence the final cessation of osteoclast resorption. The hormones calcitonin, vitamin D_3 (1,25 Vit D_3), parathyroid hormone (PTH), and estrogen all have a function in osteoclast activity, differentiation, regulation and, ultimately, cessation of osteoclast resorption (Crockett et al., 2011). Calcitonin is secreted from the parafollicular cells of the thyroid gland, and, when it is inhibited from binding to its osteoclastic cellular receptors, there are significant downstream intracellular effects. These include reductions in ruffled border amount, inhibition of endocytosis of bone and mineral at the ruffled border, and a reduction in osteoclast number over time (Chambers & Magnus, 1982; Stenbeck, Lawrence, & Albert, 2012; Zaidi, Inzerillo, Moonga, Bevis, & Huang, 2002). As previously mentioned, nitrogen-containing bisphosphonates such as zoledronate have very specific intracellular effects through action on the FPPS pathway within the osteoclast cell.

The Hindlimb Unloading Model

The present study used the hindlimb unloading mouse model to mimic microgravity-like weightlessness. In effect, the model induces musculoskeletal disuse in mouse hindlimbs. The model is a longstanding, validated, rodent-specific one used to mimic the musculoskeletal effects experienced during spaceflight (Morey-Holton & Globus, 1998). Adult mice incur a net loss of bone during both spaceflight and in hindlimb unloading ground analog model. Much of the early research related to bone in spaceflight used young, pubescent rats,

which presented with a halt to bone growth rather than a net loss of bone (Globus & Morey-Holton, 2016).

Hindlimb suspension allows for unrestricted forelimb movement. The model does not produce excessive stress to the animals, as demonstrated by bodyweights of HU mice remaining similar to those of control animals (Morey-Holton & Globus, 2002). Similar skeletal structural changes due to aging occur in both mice and humans; thus, mice are an appropriate model to understand age-related bone losses (Ferguson et al., 2003; Halloran et al., 2002).

Mice from 3 to 6 months of age are considered mature and postpubescent. This age range is physiologically comparable to humans between 20 and 30 years of age (Flurkey, Currer, & Harrison, 2007). Postpubescent mice of 16 weeks were used in the present study. The age of the mice at the end of the 3 week study placed their age group analogous to humans in their middle 20's. Astronauts from the National Aeronautics and Space Administration (NASA) have an age range for their astronaut corps between 25 and 55 years (Orwoll et al., 2013).

Mechanical Testing and the Three-point Bending Configuration

Bending tests are useful for assessing the mechanical properties of rodent bones. The small size of mouse femurs makes machine working of specimens difficult. Bending tests centered on a diaphyseal section of the mouse femur are common in the literature (Jepsen et al., 2015). The mass of bone at the

diaphysis is predominately cortical bone. The bone receives a monotonic load at a certain rate of displacement to induce bending until the specimen fractures (Fyhrie & Christiansen, 2015). Bending tests cause the side receiving the applied force to experience compression, while the opposite side experiences tension. Bone is weaker in tension and usually fails on the tensile side first (Turner & Burr, 1993). Figure 2 provides an illustration representing the 3-pt bend test.

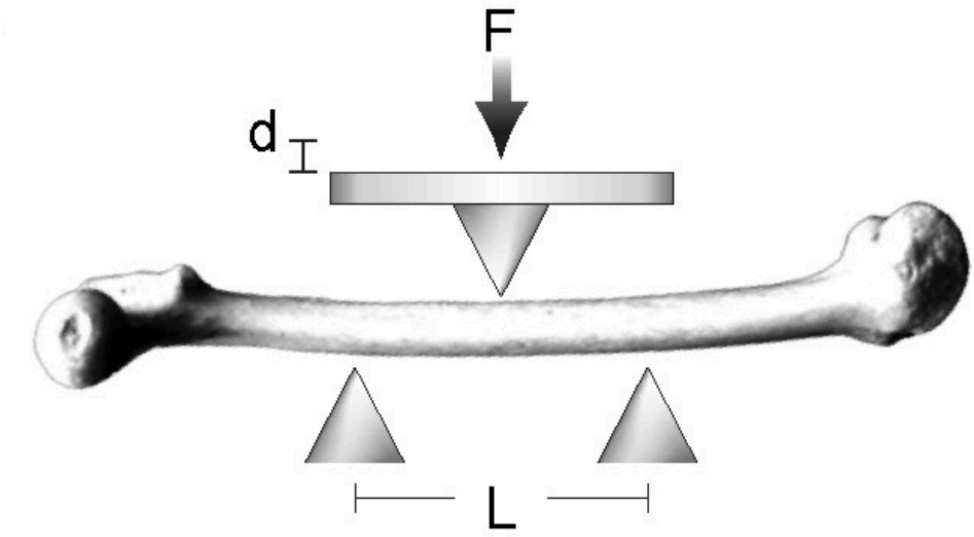

Figure 2. Three-point bending configuration. Configuration of the 3-pt bend test along the diaphysis of the femur. *F* is the direction of the force applied, and *d* is the resulting displacement (mm) from beginning of force application until completion of test. The test is performed at exactly midpoint of the span length of the pins (5 mm), signified by *L*, just inferior to the third trochanter. Data collected from this test report the force and displacement measurements until the bone fully fractures.

Precise reporting of subject and testing apparatus dimensions is crucial to enable accurate comparisons across studies. An important consideration of the 3-pt bend test is the orientation of the femur either anterior-posterior or posterior-anterior. Opposing sides of the in vivo mouse are subjected to differing stresses from the insertion and actions of muscles and vector of gravity. This results in differing strength properties of the tested bone on different sides of the femur (Jepsen et al., 2015). Table 1 summarizes the literature for pertinent bending studies. Of the 15 studies examined that reported these data, eight had femurs presented with the anterior surface facing down and seven had femurs presenting the reverse. The femur was positioned anterior face down for this study. This was intended to expose the anterior face of the femur to failure from applied forces first (in tension).

Another important detail of the test is the span length between the bottom two supports. Based on the need to apply beam theory equations to arrive at tissue-level properties, a section of the femur most cylindrical was necessary (Gere & Timoshenko, 1984; Turner & Burr, 1993). A 5 mm span width between the two bottom supports was chosen just distal to the third trochanter on the lateral border of the femur. This choice agrees with literature (Akhter et al., 2000; Akhter, Fan, & Rho, 2004). During this study, calipers were used to ensure precision.

Table 1

Femur Bending Methods

Animal	Type	Orientation	Span Length	Load Rate (mm/s)	Reference
Rat	4 point	Ant-Post	not reported	0.5	Bonadio et al. (1993)
Mouse	3 point	Ant-Post	5 mm	0.05	Akhter et al. (2000)
Rat	3 point	Post-Ant	13 mm	0.166	Ferretti et al. (1993)
Rat	4 point	Ant-Post	not reported	0.5	Smith et al. (2000)
Mouse	3 point	Post-Ant	7 mm	0.3	Silva et al. (2006)
Mouse	3 point	Ant-Post	6.5 mm	0.155	Jämsä et al. (1998)
Mouse	4 point	Post-Ant	4 mm	0.033	Brodt et al. (1999)
Mouse	3 point	Ant-Post	5 mm	0.05	Akhter et al. (2004)
Mouse	3 point	Post-Ant	7 mm	0.033	Wergedal et al. (2002)
Mouse	3 point	Ant-Post	10 mm	0.2	Schriefer et al. (2005)
Rat	3 point	Ant-Post	not reported	0.1	Ke et al. (1998)
Mouse	3 point	Ant-Post	6 mm	0.5	Voide et al. (2008)
Mouse	3 point	Post-Ant	10 mm	0.033	Spatz et al. (2013)
Mouse	3 point	not reported	8 mm	0.0833	Lloyd et al. (2008)
Rat	3 point	Post-Ant	13 mm	0.166	Ferretti et al. (1993)
Mouse	3 point	not reported	4 mm	0.166	Kodama et al. (2000)
Mouse	3 point	not reported	5 mm	0.5	Turner et al. (2000)
Mouse	3 point	Post-Ant	7 mm	0.033	Wergedal et al. (2005)

Whole-bone mechanical properties are based on forces applied and displacement incurred on a specimen. A force-displacement curve may be graphed from the data and divided into two distinct regions: the elastic deformation and plastic deformation regions (Figure 3). The initial slope of the curve of the elastic region is known as stiffness (N/mm), a measure of how much a bone can deform without sustaining permanent deformation. The bone deformation is transient; it returns to its original shape. The elastic and plastic regions of the force-displacement curve are divided by a yield point, N. This is the peak of the initial linear stiffness slope when forces on the bone result in microcracks such that permanent damage occurs. The point where a bone can sustain the greatest force is the ultimate force (N). Postyield displacement (PYD) is a measurement of the amount of permanent deformation prior to fracture. Finally, there is a fracture point force, which is where the last of the force is applied before a complete fracture of the bone (Jepsen, Pennington, Lee, Warman, & Nadeau, 2001; Turner & Burr, 1993).

The size of the bone tested is of critical importance for reliable whole bone mechanical tests. Tissue-level mechanical properties of bone are size-independent, enabling two different bones to be compared (Jepsen et al., 2015). This is accomplished by converting the raw force-displacement data into a tissue-level stress-strain curve by using mechanical engineering equations, which are shown in Figure 4 (Gere & Timoshenko, 1984; Turner & Burr, 1993).

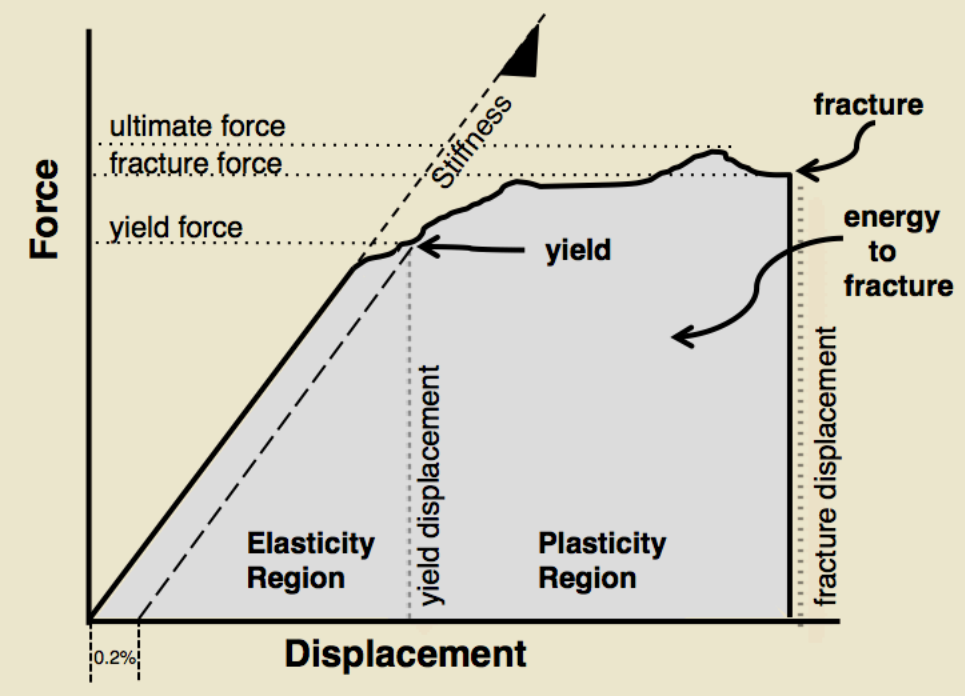

Figure 3. Force-displacement curve. Mechanical properties and notable attributes from the force-displacement curve produced by a 3-point bending test.

$$\sigma = \frac{FLc}{4I} \qquad \varepsilon = \frac{12cd}{L^2} \qquad E = \frac{F}{d}\frac{L^3}{48I}$$

Figure 4. Beam theory equations for estimating bone material properties from bending tests. Stress (*σ*, sigma, force/area) is the applied load per unit of cross-sectional area. Strain (*ε*, epsilon, [elongated length – original length]/original length) is the measurement of percent change in length, or relative deformation. Elastic modulus (E, N/mm^2 = MPa, megapascal) is the resistance to permanent deformation at a tissue-level, and corresponds with the whole-bone parameter of stiffness. *F* is applied force, *d* is displacement, *L* is span length, *c* is the distance from the center of mass, *I* is the cross-sectional moment of inertia.

The whole-bone displacement (mm) or tissue-level strain (%) beyond the yield point up until the fracture point is a measurement of the ductility of a material (Jepsen et al., 2015) (Figure 3). When a material lacks much postyield region, it is referred to as a brittle material. Chalk is an example of a brittle material with little plasticity. In a brittle material, once the elasticity of the material is breached at the yield point, very little energy is required for fracture failure. The area under the force-displacement curve is a measurement of energy, known as work-to-fracture (Nmm; toughness) (Jepsen et al., 2001, 2015; Turner & Burr, 1993). The postyield displacement, postyield strain, and work-to-fracture (toughness) were all examined in this study.

Structural Imaging of Bone Morphometry

It is important that the materials and geometric morphometry of bone specimens are analyzed along with mechanical testing. The structure influences the mechanics. The structural measurements of cortical and cancellous bone were measured for this study, and established guidelines for micro-computed tomography (μCT) were taken into consideration (Bouxsein et al., 2010). In this study, μCT evaluated bone morphology and microarchitecture ex vivo. Data were acquired of the attenuation of X-rays from multiple angles. These data were then compiled to reconstruct 3-dimensional images that represented the spatial and density characteristics of the material. Bone is a composite material of both inorganic and organic components. The method of μCT specifically elucidates a bone's structure and morphology with X-rays attenuating through the

inorganic phase of calcium-phosphate in the form of semi-crystalline HAP with carbonate, accounting for 35-45% of bone volume. The other primary components of bone are collagen, with its enzymatic and nonenzymatic crosslinks (35-45% bone volume) as well as water (15-25% bone volume) (Granke, Does, & Nyman, 2015). Both 2-dimensional (2D) and 3-dimensional (3D) μCT architecture were examined in this study, translating into both volume and areal outcomes.

Chapter III

Methods

This study was conducted in the Bone and Signaling Laboratory at the NASA Ames Research Center. The purpose of the study was to assess bone properties in the presence of zoledronate and simulated weightlessness. This was accomplished through software analysis of bone geometry from μCT scans, ex vivo mechanical testing, and utilization of mechanical engineering equations for tissue-level material properties.

Ethics Statement

All animal experimental procedures were approved by the Institutional Animal Care and Use Committee at the NASA Ames Research Center (protocol NAS-13-004-Y1), with tissue use approved by the San José State University Institutional Animal Care and Use Committee (protocol 2015-E). All animal handling procedures were followed according to the U.S. National Institutes of Health Guide for the Care and Use of Laboratory Animals (National Research Council (US) Committee for the Update of the Guide for the Care and Use of Laboratory Animals, 2011).

Animals and Study Design

Thirty-two male, postpubescent, 16-week-old C57BL/6 mice (Jackson Laboratory, Bar Harbor, ME) were housed at the NASA Ames Research Center. The animals were randomly divided into four groups (n = 8). Body mass (g) was measured and used to distribute mice evenly throughout the four groups. In the

ambulatory group (NA), eight were injected with saline vehicle (VEH) while another eight were injected with the same volume of zoledronate (ZOL, 45 μg/kg, from Sigma Aldrich). In the hindlimb unloaded (HU) group, eight received saline vehicle (VEH) while another eight received the same volume of ZOL (45 μg/kg). The subcutaneous injections were performed at the lower back 3 days prior to hindlimb unloading, with these days also serving as the cage acclimation period. All animals were monitored at least twice a day, maintained on a 12/12 light/dark cycle (6 am to 6 pm). The mice were given standard laboratory food chow (Lab Diet 5001, Purina Mills, St. Louis, MO) and water ad libitum throughout the duration of the study. Normal behavior of grooming and trauma-free coats were observed.

Hindlimb Unloading

The HU group underwent 3 weeks of hindlimb disuse according to the method of Morey-Holton and Globus (2002). This technique suspended the animal at 30° with tail traction while permitting free movement of the forelimbs. Mice in the NA group were individually housed for the same period of time to mimic the isolated stress of the HU group.

It is of note that in a separate component of this study we utilized the same mice and investigated the effects of in vivo mechanical loading on the right tibia in conjunction with ZOL and HU administration. All of this study's animals underwent applied mechanical loading to their right tibias three times a week for 3 weeks. While anesthetized, mechanical loading involved a 9N pulse in

compression (~1300 μstrain), applied 60 times with 5 s intervals on the mouse knee, transmitting force uniaxially through the tibia to the stationary positioned calcaneus. The entire process of anesthetization, loading, recovery, and immediate return to HU lasted, on average, 12 min per loading session. Mice were removed from the HU apparatus during compression application, which was administered after mice were anesthetized with 2% isoflurane. Additionally, each animal in this study had its left tibia analyzed via dynamic and static histomorphometry ex vivo.

At the time of dissection, animals were momentarily ambulatory during anesthetization, with subsequent euthanizing via CO_2 inhalation. Left femurs were wrapped with PBS-soaked gauze (with calcium and magnesium chloride) and stored at -20ºC.

Microcomputed Tomography (μCT) Scanning

Prior to scanning, femurs were permitted to thaw at 4°C overnight in PBS, with an additional acclimation time of 20 min prior to scanning at room temperature. All left femurs were scanned using μCT to quantify the 2D and 3D microarchitecture (SkyScan 1174 μCT scanner, Kontich, Belgium). All whole left femurs were scanned at the low resolution isotropic voxel size of 17.3 μm per pixel to provide cortical bone data from the midsection of each diaphysis. To investigate cancellous bone, all distal metaphyses sections were scanned at the high resolution isotropic voxel size of 6.7 μm/pixel. Specimens were mounted into the low density X-ray scanner, with the bone fixed within an Eppendorf tube.

To ensure hydration during the scan, PBS-soaked gauze was wrapped around the femurs. A 0.5 mm aluminum X-ray filter was affixed in the line of sight between the X-ray source and the specimen, with the X-ray beam scanner operating at 50 kV and 800 μA. Scan settings were set to an exposure time of 3.5 s per frame, with the images averaged across two captured frames for every rotated step of 0.5° and the bone rotating throughout an entire angular span of 180°.

Reconstruction

Scans were reconstructed into 2D cross sections using the software NRecon (SkyScan, v.1.6.10.2). Dynamic range settings across all samples were consistent after the upper limit of the linear attenuation coefficient threshold was determined to be 0.15. Reconstruction parameters additionally included a beam hardening correction of 30% and a ring artifact correction of 4.

Morphometric Analysis

Two rotational alignment protocols were developed to quantify the morphometric data from the mid-shaft diaphysis and the distal metaphysis. Using the reconstructed images, the low and high resolution femoral images were aligned to ensure a consistent rotation in the coronal, sagittal, and transverse planes across all samples using the SkyScan software DataViewer (v.1.5.2, Figure 5). The distal growth plate and greater trochanter were selected as consistent anatomical landmarks for the low-resolution, whole femur protocol. This ensured that the diaphyses were parallel in the Y-axis and the cortical bone

was upright in the Z-axis, enabling accurate moment of inertia data for postprocessing analysis. A similar protocol was devised for consistency in the high resolution images of the distal metaphysis. Before the regions of interest were selected for contouring, a lower and upper threshold of the foreground from the background into a binary image indicating bone was determined using 15 samples. The selected values were used across all samples in the SkyScan CT-analyser software (CTAn, v.1.10). This point in the imaging process was also where the pixelization of the scans was analyzed quantitatively to determine tissue mineral density (TMD).

For the 6.7 μm/pixel scans, the distal metaphysis volume of 1500 μm was contoured, based on a 410 μm offset from the growth plate. For the 17.3 μm/pixel scans of the whole femur, a 5 mm span width was identified for use in the 3-pt bending tests in DataViewer starting at the most distal portion of the third trochanter of the mouse where cortical bone thickness contours were uniform.

Measurements

The program ImageJ was used to increase the accuracy of bone placement upon the pins. Based upon imaging, all samples were labeled for a 5 mm span descending inferiorly from the third trochanter. This method ensured precise femur placement to increase the reliability of mechanical testing (Figure 6).

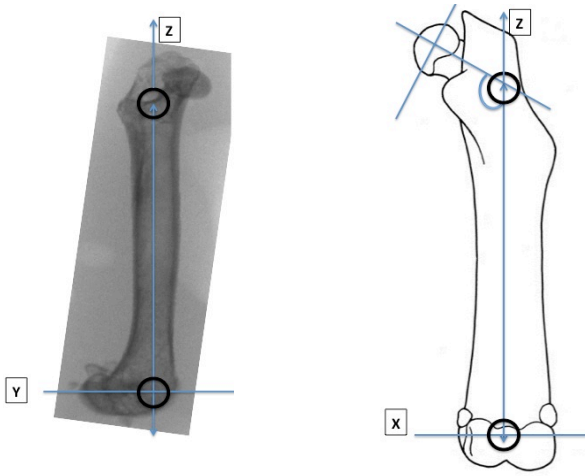

Figure 5. DataViewer protocol of mouse femoral scans. Sagittal femur view on left and coronal femoral representation on right. A protocol was developed to ensure consistent positions across all µCT samples with regard to 2D measurements and, especially, the moments of inertia. Notice the condyles of the femur presenting in both views inferiorly, with the femoral head and greater trochanter presenting superiorly. Take note of the X, Y, Z orientations which were adhered to across all subject scans based on the growth plate center, diaphysis, femoral neck, and greater trochanter.

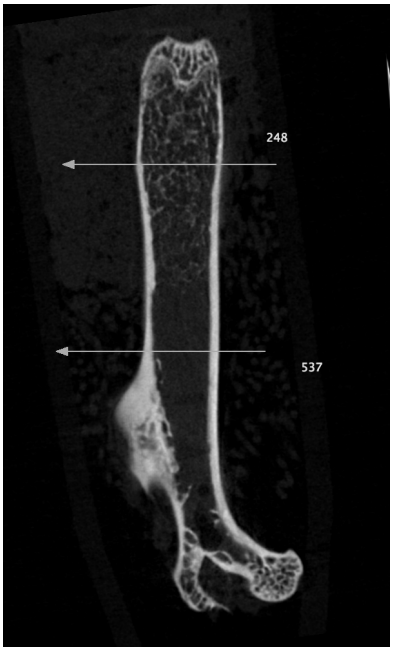

Figure 6. Coronal view of ImageJ mouse femoral scan.

Mechanical Testing

Monotonic 3-pt bending mechanical tests to failure were conducted on all left femurs at a constant displacement rate of 0.01 mm/s (Bose ElectroForce 3220 Series II with 225 N load cell; Bose Corporation, Eden Prairie, MN, USA). Determination of 5 mm and 1 mm sections of the femoral diaphysis was made by examination of the 17.3 μm/pixel low resolution images. ImageJ was used to create high resolution image files to increase the accuracy of specimen placement on the lower two spans. On the evening prior to mechanical testing, the femurs were transferred from a -20°C to a 4°C freezer. Samples were allowed 20 min for thawing in room temperature (25°C) PBS. The anterior surface of the femur was placed in contact with the lower two pins, with a 5 mm span between pins. Calipers were used to ensure accuracy (Figure 7).

Statistical Methods

All statistical analyses were performed using JMP (v.8, SAS Institute, Cary, NC). To enhance accurate analysis of the treatment groups on the bone structure and mechanical indices, the influence of body mass was taken into consideration. A linear regression with two independent variables (HU/NA, ZOL/VEH) and a bodyweight variable was conducted. All interactions were analyzed between all parameters (HU, NA, ZOL, VEH, BW). If there were no interactions with bodyweight (homogeneity of regressors), then interactions were removed and a two-way ANCOVA was performed. The least squares means and standard deviations are reported.

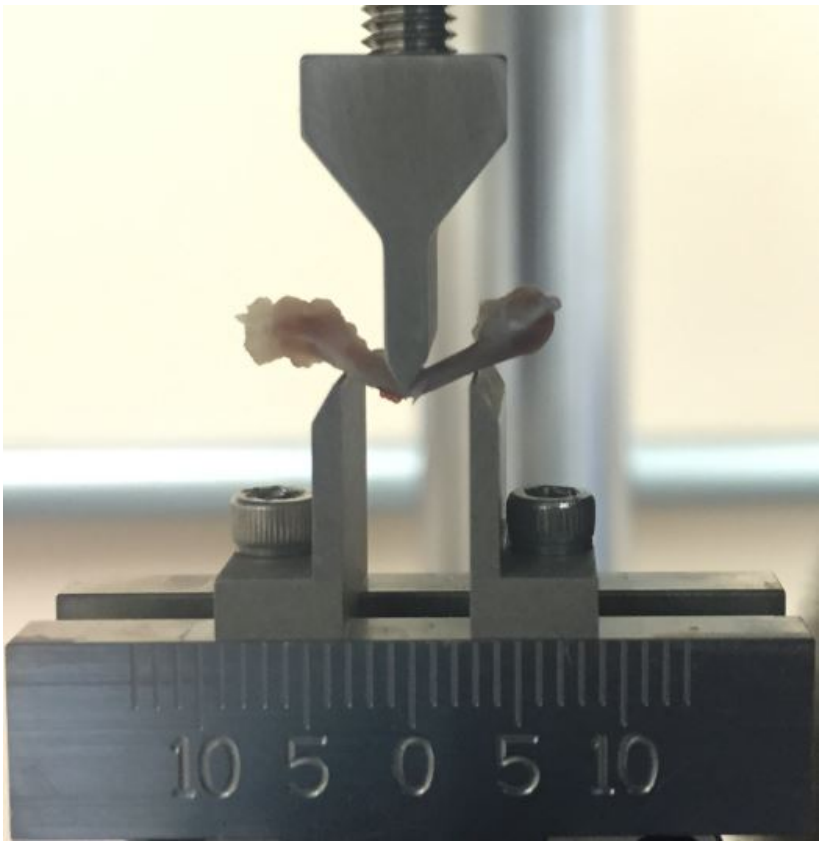

Figure 7. Lateral view of three-point bending test apparatus. Notice the condyles on the right side of the mouse femur facing upwards.

Chapter IV

Results

This study investigated the effects of zoledronate on bone mechanical and structural properties during simulated weightlessness as a model of spaceflight. It was hypothesized that the zoledronate-treated mice experiencing simulated weightlessness would increase their whole-bone elastic stiffness but have a diminished mechanical plasticity, making the bone more brittle and less tough.

Bodyweight Analysis

Throughout the study, mice were weighed twice a week to monitor bodyweight. At the onset, body mass was measured and used to distribute mice by weight evenly throughout the four treatment groups. After a 3-day acclimation period, the weight on the first day of HU was taken as the basal bodyweight (g), and the measurement during the last week of HU was taken as the final bodyweight (Day 17). As shown in Figure 8, bodyweight was significantly lower in HU animals from basal to final bodyweight (-10.5%) compared to NA controls (-3.1%, $p = 0.0001$). No changes were observed after ZOL treatment. This impactful relationship of body mass and HU treatment necessitated use of the general linear model of analysis of covariance (ANCOVA). Treatment effects were analyzed with bodyweight as the covariate. In terms of bodyweight, these data suggest that a certain aspect of hindlimb unloading resulted in bodyweight changes. Hindlimb unloading itself may have caused less feeding due to stress,

or perhaps the anesthesia administration in combination with axial compressions on the right tibia induced systemic stress as well.

In the review of the 3-pt bending test data, results from five animals were missing during the tabulation and data transformation process. The final sample sizes for the mechanical testing ANCOVA process were: NA/VEH: 6, NA/ZOL: 7, HU/VEH: 7, and HU/ZOL: 7.

The mid-diaphyseal cortical μCT data had four datasets with substantial visual streaks obscuring scans and reconstruction noise, and one sample was fractured near the diaphyseal midpoint during dissection. Those data were removed, and the final sample sizes for the μCT cortical structure ANCOVA process were: NA/VEH: 6, NA/ZOL: 7, HU/VEH: 7, and HU/ZOL: 7.

A few samples were removed for reconstruction noise and μCT scan streaks from the distal metaphyseal cancellous datasets. Additionally, a final review prior to ANCOVA showed a single animal's cancellous parameters exhibiting abnormally high results in bone volume fraction, BV/TV; trabecular thickness, Tb.Th; and trabecular number, Tb.N. This animal was in the NA/VEH group. A Grubbs Extreme Studentized Deviate Test categorized the BV/TV results for this animal as an outlier ($p > 0.05$). The same animal presented with normal bone levels in its cortical μCT scan. Only cancellous data for that animal were removed. The final sample sizes for the μCT cancellous structure ANCOVA process were: NA/VEH: 5, NA/ZOL: 7, HU/VEH: 7, and HU/ZOL: 6.

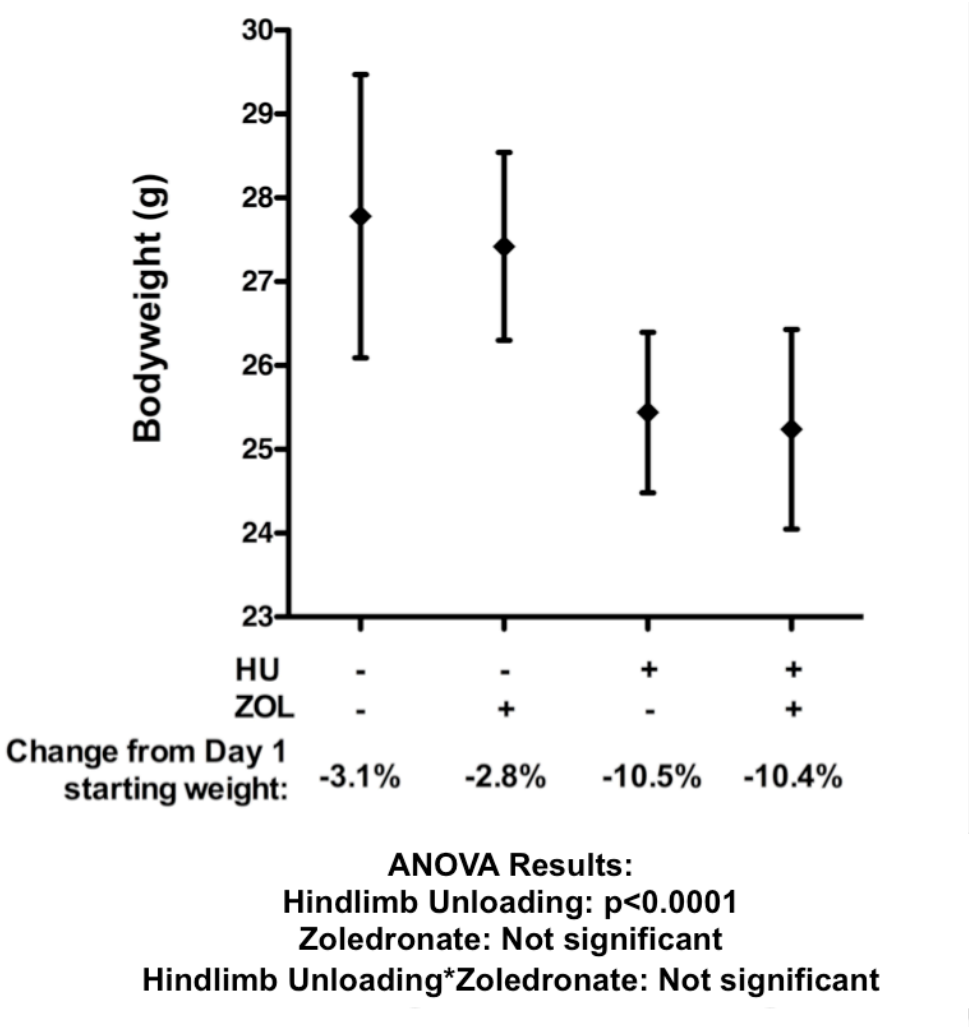

Figure 8. Final bodyweight analysis. Weight on day 17, during the last week of unloading. Values are *M* ± *SD*.

Cancellous Structure, Tissue Mineral Density

Cancellous structure and tissue-level density of the distal femoral metaphysis were measured by μCT (6.7 μm/pixel). As a main effect, ZOL improved the cancellous tissue at this region for each parameter over VEH (*p* =

0.001, Table 2). Relative to vehicle, ZOL increased the bone volume fraction (BV/TV) by 7% and tissue mineral density (TMD) by 8%. An interpretation of these data confirms the efficacy of ZOL for maintaining bone structure and mineral content in the distal femoral metaphysis by preventing bone resorption via osteoclast inhibition or perhaps in conjunction with prevention of osteocyte apoptosis, a topic still being investigated (Plotkin, Bivi, & Bellido, 2011).

Hindlimb unloading had no statistically significant main effect, despite a 28% BV/TV reduction in the vehicle-treated group. A subsequent analysis revealed there was a lack of statistical power via loss of animals and the ANCOVA process to homogenize the regressor relationship. Testing the assumption of homogeneity of regressors for HU and bodyweight in the ANCOVA process presented with two trends toward an interaction for trabecular separation (p = 0.07) and trabecular number (p = 0.09). This indicates a trend toward an interaction effect of HU by bodyweight in the VEH animals but not in ZOL. A post-hoc power analysis was performed, and a sample size of 11 would have been needed to detect this difference for trabecular number with 80% power. Taken together, these data suggest that bodyweight losses influenced the skeletal response to disuse in the cancellous tissue, with ZOL preventing bone loss.

Table 2

Structural Results for Cancellous Bone with μCT

	Normal Ambulatory		Hindlimb Unloading		Effects Test		
	Vehicle	Zoledronate	Vehicle	Zoledronate	ZOL	HU	ZOL*HU
Bone Volume Fraction (%)	13.31 ± 4.1	19.33 ± 3.5	9.59 ± 3.6	19.29 ± 3.8	0.0001	0.38	0.17
†Trabecular Separation (mm)	0.208 ± 0.023	0.187 ± 0.019	0.219 ± 0.020	0.182 ± 0.021	0.001	0.79	0.27
Trabecular Thickness (mm)	0.054 ± 0.005	0.063 ± 0.004	0.049 ± 0.004	0.061 ± 0.005	0.0001	0.20	0.37
†Trabecular Number (1/mm)	2.41 ± 0.53	3.00 ± 0.46	1.90 ± 0.47	3.13 ± 0.50	0.0001	0.49	0.07
Mineral Density (mgHA/cm^3)	0.371 ± 0.017	0.402 ± 0.014	0.355 ± 0.015	0.395 ± 0.016	0.0001	0.19	0.32

Note. Least Squares Mean Adjusted data are presented as *M* ± *SD*. Parameters met the homogeneity of regressors criteria for ANCOVA with body weight as covariate. Significant p-values included for ANCOVA results. †Parameters found to have a trend toward not having homogeneity of HU treatment regression slopes in terms of body weight. Trabecular Separation, HU*BW = 0.07. Trabecular Number, HU*BW = 0.09.

Cortical Structure, Tissue Mineral Density

Cortical architecture and mineral density at the subtrochanteric femoral diaphysis were measured by μCT (17.3 μm/pixel). With no significant impact on cortical TMD, ZOL significantly increased cortical thickness (p = 0.007, Table 3), though with only a marginal biological increase of 2% compared to VEH.

Hindlimb unloading had no statistically significant main effects, despite a 10% cortical thickness reduction in the VEH group, indicative of a bodyweight contribution. Interestingly, HU presented with two statistical trends toward an effect for cortical bone area (p = 0.07) and the polar moment of inertia, J (p = 0.06). These trends indicate that simulated weightlessness tended to both decrease cortical bone area and decrease the resistance to bending. As a combined treatment, ZOL and HU resulted in a statistically significant interaction with ZOL offsetting the trend of HU cortical thickness losses (p = 0.04). Taken together, ZOL conferred cortical thickness protection from losses in HU mice.

Table 3

Structural Results for Cortical Bone with μCT

	Normal Ambulatory		Hindlimb Unloading		Effects Test		
	Vehicle	Zoledronate	Vehicle	Zoledronate	ZOL	HU	ZOL*HU
Cortical Thickness (mm)	0.229 ± 0.017	0.233 ± 0.016	0.208 ± 0.016	0.238 ± 0.017	0.007	0.31	0.04
Cortical Bone Area (mm^2)	1.07 ± .11	1.09 ± 0.10	0.92 ± 0.10	1.04 ± 0.11	0.07	0.07	0.20
Marrow Area (mm^2)	1.15 ± 0.20	1.18 ± 0.19	1.20 ± 0.19	1.08 ± 0.19	0.55	0.78	0.31
Moment of Inertia, X (mm^4)	0.18 ± 0.03	0.19 ± 0.03	0.15 ± 0.03	0.17 ± 0.03	0.18	0.15	0.87
Moment of Inertia, Y (mm^4)	0.41 ± 0.09	0.43 ± 0.08	0.35 ± 0.08	0.38 ± 0.08	0.39	0.21	0.72
Moment of Inertia, J (mm^4)	0.59 ± 0.12	0.62 ± 0.11	0.50 ± 0.11	0.56 ± 0.14	0.47	0.06	0.29
Mineral Density ($mgHA/cm^3$)	0.77 ± 0.047	0.80 ± 0.044	0.81 ± 0.045	0.82 ± 0.046	0.20	0.21	0.58

Note. Least Squares Mean Adjusted data are presented as *M* ± *SD*. All parameters met the homogeneity of regressors criteria for ANCOVA with body weight as covariate.

Mechanical Properties, Stiffness, Plasticity

Mechanical properties were determined using 3-pt bending tests of mice femurs, and the data were analyzed at both whole-bone (mechanical properties) and tissue levels (material properties, transformation by geometry). Table 4 presents results for each parameter. Figure 3 is a generalized force-displacement curve. Figures 9, 10, and 11 are graphical illustrations of treatment main effects and combined treatment effects. For whole bone elastic parameters, HU decreased stiffness (-30%, $p = 0.05$) compared to the NA control condition (Figure 9). In contrast, ZOL increased bone stiffness (+28%, $p = 0.0001$) compared to vehicle (Figure 10). These data indicate that the dosage of ZOL was effective in inducing an increase in stiffness; additionally, even in the ANCOVA model, HU was effective in inducing stiffness losses. For stiffness, the statistically significant interaction of HU and ZOL ($p = 0.04$, Figure 11) showed the protective effect of ZOL in the presence of HU.

Taking geometry into account for tissue level parameters, ZOL resulted in an increase in elastic modulus (+17%, $p = 0.01$, Table 4). Generally, stiffness (whole bone) and elastic modulus (tissue level) parameters are analogous and parallel measures of the ability of bone to absorb forces prior to suffering permanent deformation. Interestingly, the elastic modulus showed no statistical main effect of HU compared to NA nor an interaction of HU and ZOL (Table 4). When the whole bone stiffness value was transformed its tissue level equivalent, the results indicated that geometry was a factor in the HU stiffness effect

compared to NA. In contrast, ZOL affected both whole bone and tissue level (material) changes compared to VEH in terms of stiffness and elastic modulus.

Compared to VEH, ZOL increased yield force (+11%, $p = 0.01$, Figure 10) as well as ultimate force (+17%, $p = 0.0004$), with a trend for ultimate stress, or force per unit of bone area (+11%, $p = 0.06$). Hindlimb unloading resulted in a trend ($p = 0.07$, Figure 9) of reducing yield force, yet not yield stress, compared to NA. This trend of HU reducing yield force was in agreement biomechanically with the result of HU reducing stiffness and indicated the geometric effect of HU and a material effect for ZOL. These data confirm the hypothesis for elastic stiffening.

In terms of plasticity on the whole bone scale, HU increased postyield displacement compared to NA (+20%, $p = 0.03$, Figure 9). Zoledronate did not increase postyield displacement, nor did ZOL significantly increase postyield strain at the tissue level, both compared to VEH. This provides evidence to reject the hypothesis that an increase in stiffness from ZOL would also result in a decrease in plasticity. In fact, ZOL increased the total energy (work-to-fracture) by 15% compared to VEH ($p = 0.001$), and this ZOL effect was also found for postyield energy (+16%, $p = 0.001$). Taken together, these results indicate that ZOL had a significant impact on increasing stiffness, yield force, and ultimate force without affecting the plastic displacement. These increases in mechanical properties seem to be the driving factors for the induced increases in both total and postyield energy.

Table 4

Mechanical Properties of Femoral Diaphysis with Three-point Bending

	Normal Ambulatory		Hindlimb Unloading		Effects Test		
	Vehicle	Zoledronate	Vehicle	Zoledronate	ZOL	HU	ZOL*HU
Stiffness (N/mm)	75.13 ± 12.7	96.18 ± 12.2	53.37 ± 12.1	93.25 ± 12.6	0.0001	0.05	0.04
Yield Force (N)	8.16 ± 1.7	9.09 ± 1.6	5.86 ± 1.6	8.29 ± 1.7	0.01	0.07	0.21
Ultimate Force (N)	12.88 ± 1.9	15.17 ± 1.8	11.20 ± 1.8	14.42 ± 1.9	0.0004	0.2	0.48
†Fracture Force (N)	9.69 ± 1.8	6.55 ± 1.8	6.37 ± 1.8	7.76 ± 1.9	0.26	0.18	0.007
Postyield Displacement (mm)	1.24 ± 0.27	1.25 ± 0.25	1.49 ± 0.25	1.58 ± 0.26	0.58	0.03	0.66
Total Energy (Nmm)	12.3 ± 2.4	14.2 ± 2.3	11.5 ± 2.3	15.8 ± 2.4	0.001	0.7	0.15
Postyield Energy (Nmm)	11.8 ± 2.4	13.7 ± 2.3	11.1 ± 2.3	15.4 ± 2.4	0.001	0.66	0.15
Elastic Modulus (N/mm^2)	1160 ± 396	1361 ± 379	899 ± 378	1455 ± 391	0.01	0.65	0.19
Ultimate Stress (N/mm^2)	58.4 ± 13.0	64.9 ± 12.5	55.5 ± 12.4	66.6 ± 12.9	0.06	0.9	0.6
Fracture Stress (N/mm^2)	37.8 ± 10.5	33.6 ± 10.5	31.2 ± 10.0	35.0 ± 10.3	0.94	0.6	0.27
Ultimate Strain (mm/mm)	0.109 ± 0.02	0.131 ± 0.02	0.146 ± 0.02	0.113 ± 0.02	0.43	0.36	0.001
Postyield Strain (mm/mm)	0.382 ± 0.09	0.392 ± 0.08	0.436 ± 0.08	0.474 ± 0.09	0.45	0.12	0.64

Note. Least Squares Mean Adjusted data are presented as *M* ± *SD*. Parameters met the homogeneity of regressors criteria for ANCOVA with body weight as covariate. Significant p-values included for ANCOVA results. †Parameter did not have treatment slope homogeneity with body weight. ZOL*BW = 0.02, HU*ZOL*BW = 0.04.

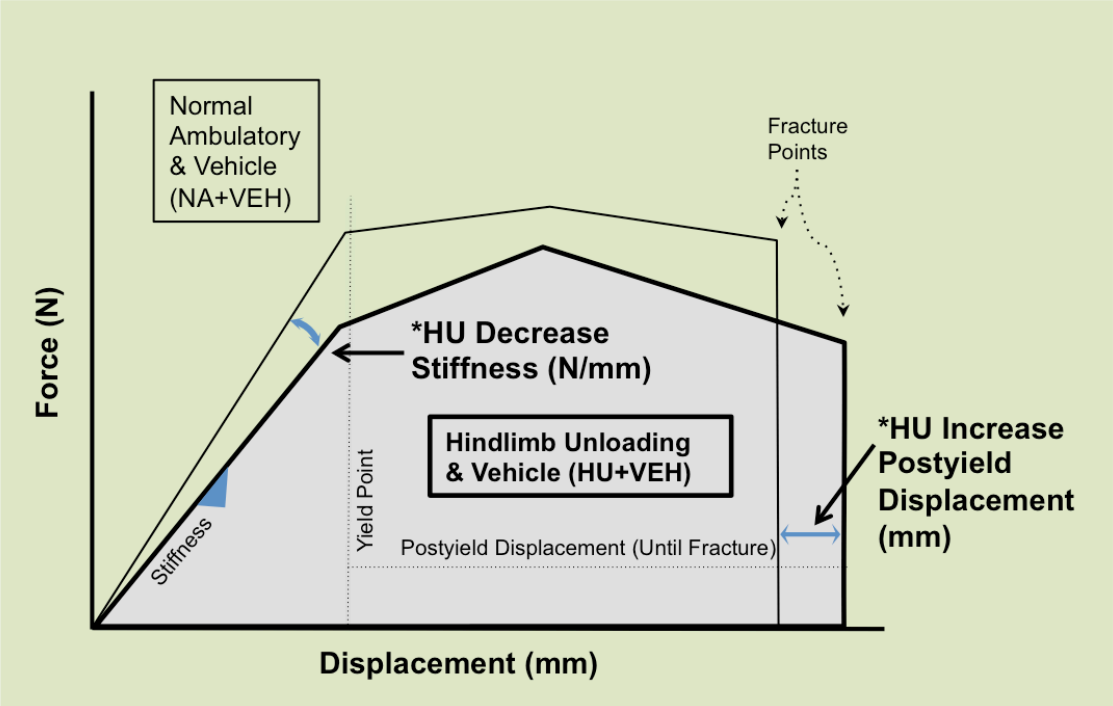

Figure 9. Hindlimb unloading mechanical effects.

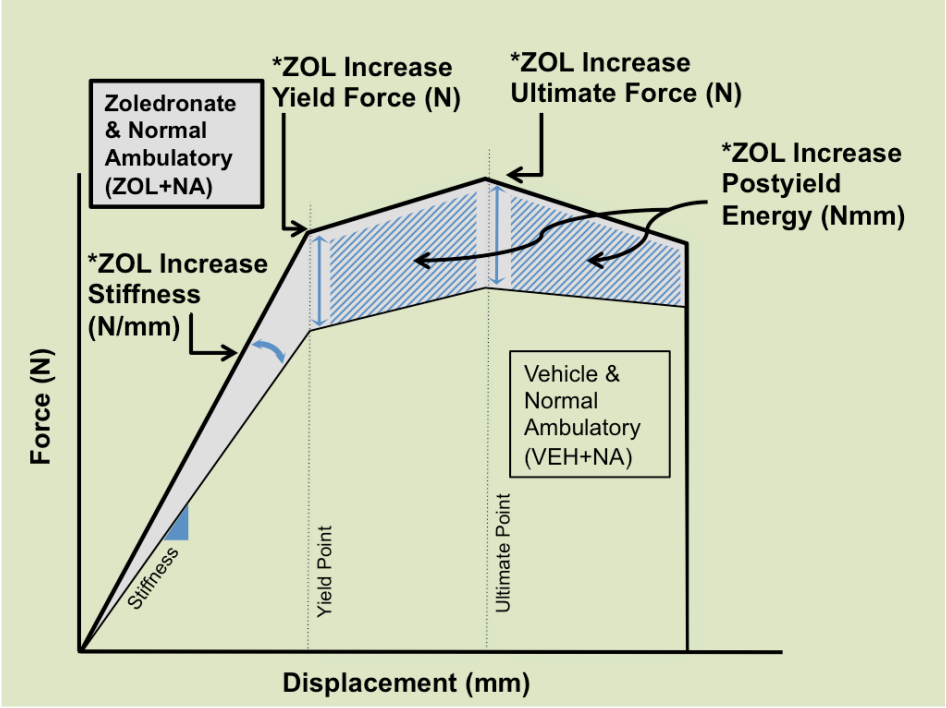

Figure 10. Zoledronate mechanical effects.

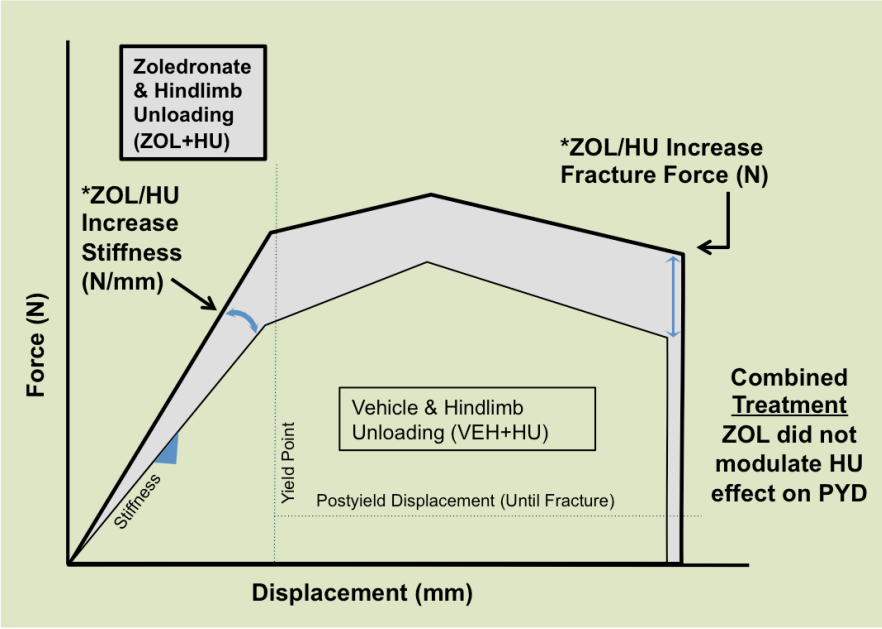

Figure 11. Combined treatment effects.

Chapter V

Discussion and Conclusions

The objective of this work was to examine the effect of zoledronate on bone mechanical and structural properties in an experimental model designed to mimic spaceflight weightlessness with a pharmaceutical countermeasure. The premise for this study was driven by the concept of Currey (2012) that bone stiffness and toughness have a relationship disallowing bone to be both very stiff and very tough at the same time. The data used by Currey were based on taxonomy and investigation of differing biomaterials to demonstrate how too much stiffness from mineralization may reduce toughness. The 30° hindlimb unloading model was used to mimic the effects of weightlessness and induce musculoskeletal disuse in mice. Structural and mechanical properties of the mouse femur were examined ex vivo. The hypothesis that zoledronate-treated mice experiencing simulated weightlessness would increase their whole-bone elastic stiffness, but have a diminished mechanical plasticity, making the bone more brittle, was not fully supported by the data. Overall, ZOL prevented negative effects of hindlimb unloading and unloading-induced bodyweight losses on structure and mechanical properties of the mouse femur.

Hindlimb Unloading Effects

In this study, we used postpubescent, 16 week old C57BL/6 male mice in hindlimb unloading to simulate weightlessness. The HU treatment decreased the stiffness of bone (-29%, Table 4). Losses of bone were also found by Lloyd and

colleagues (2008) in a similar HU model using growing female mice. Interestingly, with 2 weeks of HU in 6 week old female C57BL/6 mice, Lloyd et al. (2008) reported losses in stiffness from HU (-40%). Their loss of stiffness (in growing mice) was more severe than those in the current study (in postpubescent mice), which suggests growth suppression. This comparison provides evidence that the age, as well as gender of the mice must be closely considered when designing rodent studies. A growing bone subjected to HU is still developing and may react by inhibition of the osteoblasts responsible for bone formation. This may be due to a cross talk signal coupling effect, with a subduing of osteoblasts via osteoclast inhibition (Crockett et al., 2011; Lloyd et al., 2008; Mellis et al., 2011).

This study's finding that HU resulted in a loss of stiffness is corroborated by the marginal trending loss of cortical bone area and polar moment of inertia (Table 3), yet with no change in tissue mineral density. The ability of ZOL to prevent the loss of cortical thickness in HU animals also supports this claim. Architectural measurements of bone have been found to correlate well with mechanical properties, such as stiffness (Jepsen et al., 2015). Taken together, these results were expected. A trending effect of HU in reducing bone area and the polar moment of inertia provides an underlying mechanism for the reduced bone stiffness.

The HU mouse model has previously been shown to display early and pronounced cancellous architectural bone losses (Alwood et al., 2010; Amblard

et al., 2003; Judex et al., 2004). This is in line with losses seen in weight-bearing bones of astronauts (Collet et al., 1997; Lang et al., 2004; LeBlanc et al., 2000; Vico et al., 2000). While not statistically significant, the raw data from the current study show bone losses from HU compared to NA (Tables 2 & 3). Lower statistical power and bodyweight loss may have contributed to the lack of statistically significant results.

This effect of HU leading to greater resorption of cancellous bone due to osteoclast activity has been shown in the literature. Shahnazari et al. (2012) presented results describing the temporal-dependent activity of osteoclasts in bone resorption over the course of 4 weeks of hindlimb unloading. In 24 week old C57BL/6 mice (mature), an acute, but transitory increase of osteoclasts was found in weeks 1 and 2, with the osteoclast-to-bone surface ratio returning to normal by week 4. These results were consistent with bone volume (BV/TV) and mineral losses. The increase in osteoclasts in weeks 1 and 2 led to the significant bone and mineral losses toward the end of unloading. Iwaniec et al. (2005) showed that after 1 week of HU of two different genetic strains (Wild-Type and Transgenic $ß_1$-integrin) of young female mice (9 weeks of age), osteoclast surface area increased, consistent with a 30% reduction in cancellous bone in the distal femur.

Compared to the NA group, the other impact of HU in this study was the increase in postyield displacement, a measurement of ductility and bone plasticity (Table 4). It is worthy to mention that compared to NA, HU did not have

a statistically significant effect on for postyield strain, the concomitant tissue level measure, though the data were similar for postyield displacement. This suggests that geometrical changes, but not mineral concentration changes, contributed to the HU effect. When whole bone force-displacement values are transformed to the material level, geometry, but not mineral concentration, is factored into various stress and strain measurements. While these data allow inferences about one measurement of bone plasticity, a collagen assay would be required to determine the full array of constituents at the material level, including the ratio of matrix to mineral, the enzymatic crosslinks of collagen, and the water content (Burr, 2002).

Summarizing the effect of HU on mechanical properties, HU reduced bone stiffness, a measurement of bone's elastic ability to sustain forces in the preyield region without permanent deformation. Hindlimb unloading also resulted in an increase in postyield displacement. The postyield region, both in terms of displacement length and energy (areal) measurements, describes a bone's toughness and plasticity, respectively. Hindlimb unloading increased the displacement the bone could withstand prior to full fracture, without a significant impact on the bone's ability to absorb energy prior to fracture (total energy or postyield energy). Both postyield displacement and total energy are important factors in bone toughness. In bone biomechanics, a tougher bone is more resistant to fracture, separate from elastic behavior. On a structural level, the increase in postyield displacement seen in HU animals suggests that the bone

was able to sustain forces over a greater distance before full separation between the lamellar layers of bone. This full fracture separation has been described as a progressive accumulation of microfractures, leading to full breakage (Turner & Burr, 1993).

Throughout much of the literature, stiffness is a commonly reported value in mice and rat models. Energy absorption, toughness, and postyield displacement have received less focus, with values often not reported in biomechanical rodent studies. Attention has recently emerged for using the rodent model to investigate bone plasticity. This is, in part, attributable to evidence of reduced bone toughness as a characteristic in atypical femoral fractures, one of the clinical concerns with long-term bisphosphonate use (Shane et al., 2010; van der Meulen & Boskey, 2012).

Using the 3-pt bending method, Shirazi-Fard, Kupke, Bloomfield, and Hogan (2013) found an increase in postyield displacement after the initial 28 days of unloading in rats (6 months old) compared to ambulatory controls. It is worth noting that postyield displacement is simply one of the factors that can describe plasticity of bone. The total energy incurred on bone, also called work-to-fracture, is the total amount of energy under the force-displacement curve. Besides postyield displacement, the placement of that curve also depends on the magnitude of the yield, ultimate, and fracture forces. Shirazi-Fard et al. reported that HU for 28 days had no significant effect on energy-to-max force (the amount of energy accumulated to maximum force, the point synonymous with ultimate

force). These results closely relate to the current study, with limitations of subject selection and the selection of 3-pt bending on the tibia of the rat, not the femur of the mouse. In contrast, Jing et al. (2014) investigated the rat femur in 3-pt bend and a reduction in stiffness and total energy-to-fracture as well as reduced points of yield and ultimate force in terms of displacement after 4 weeks of HU.

Zoledronate Effects

In this study, we utilized 45 μg/kg as the dose of ZOL and examined the mechanical and structural effects on mouse bone. The objective was to replicate the dose administered in the study of C57BL/6 mice conducted by Lloyd et al. (2008). Results of the current study were in agreement; the dose of ZOL was effective in conferring positive structural and mechanical results. In the current study, ZOL greatly increased the stiffness of mouse bone over the course of 3 weeks compared to VEH, normal ambulatory, age-related controls (+28%). This stiffness increase is consistent with the +21% increase found by Lloyd et al. (2008). Zoledronate also had an effect on increasing the concomitant tissue level property of elastic modulus in the current study compared to VEH. This suggests that on the tissue level, similar elastic properties were conferred when transformed by the geometry of the bone. There are several important distinctions between the Lloyd et al. (2008) study and this project, such as age of the mice (6 vs. 16 weeks old), gender (female vs. male), and the ZOL injection latency period (2 weeks vs. 3 weeks). The selection of mature mice in the current study was designed to provide a contrast with Lloyd et al. (2008),

allowing for comparison of a similar dose of ZOL with the same genetic breed but at differing ages.

Compared to VEH, there was a statistically significant effect of ZOL on cortical bone in this study, but a biologically minimal effect in increasing cortical thickness (+2%), and cortical bone area (+2%, Table 3). Zoledronate affected all cancellous parameters (Table 2). Biologically, cancellous bone has been shown to have turnover rates about 10 times that of cortical bone, which could explain these data (Burr et al., 2003). Similar to HU expectations, it was anticipated that 3 weeks after a single ZOL injection, there would be a pronounced effect on cancellous architectural struts. Compared to VEH, the percentage of cancellous bone increased (BV/TV); the distance between struts decreased (Tb.Sep), making the bone less porous; and the thickness per strut increased (Tb.Th). ZOL increased the tissue mineral density of HAP in cancellous bone (Canc. TMD), although not in the cortical compartment.

Compelling cellular mechanistic evidence of the actions of ZOL on mice bone was provided by Kuroshima, Go, and Yamashita (2012). The authors examined long-term effects of an extremely high dosage of ZOL (100 μg/kg, two injections per week) on bone cells and bone microarchitecture in young male mice. With a starting age of 8 weeks, the dosage regimen lasted for 13 months, nearly half the lifespan of the animal. The authors confirmed that ZOL significantly decreased the osteoclast surface area of bone, with no significant effect on osteoblasts, compared to age-related controls. Through μCT, they

demonstrated that ZOL had a protective effect on both cancellous and cortical bone. Since the current study investigated the effect of ZOL on bone mineral, it is interesting to note that with the extreme duration and dosage used by Kuroshima et al. (2012), the mice did not display trabecular hypermineralization with overly high tissue mineral density values of HAP in the cancellous bone of the femoral metaphysis, consistent with the results of this study. While Kuroshima et al. (2012) demonstrated zoledronate's effect on cellularity and quantity of bone, the quality of bone was not investigated. Notwithstanding, the bones did not become hypermineralized, while increasing bone volume at the distal metaphysis. This work on the cellularity and bone architecture after long-term ZOL treatment provides neither cellular nor bone architecture support for the concept proposed by Currey (2012), which was predicated on bone brittleness resulting from hypermineralization.

The effects of ZOL on increasing cancellous bone structure in the current study are in line with previous mouse research (Lloyd et al., 2008; Pozzi et al., 2009). Compared to VEH, zoledronate has been shown to increase bone mineral density of the cancellous-rich region of the distal femoral metaphysis in rats (Smith & Allen, 2013) and the cancellous-rich bone mineral density of the tibial metaphysis in ovariectomized rats (Gasser, Ingold, Venturiere, Shen, & Green, 2008). In the current study, a ZOL dose of 45 µg/kg induced positive increases in cancellous bone and tissue mineral density compared to VEH and, to a limited degree, increases in cortical architecture. Taken together, the

structural data corroborate the mechanical effect of ZOL on increasing stiffness, ultimate force, and yield force. There were thicker, more condensed and mineralized cancellous struts that contributed to the increased elasticity, along with the slight, but significant, impact of ZOL on cortical bone.

In terms of plasticity properties, the effect of ZOL is worth close consideration. This study examined the effect of ZOL 3 weeks postinjection. Compared to VEH, ZOL did not have any effect on postyield displacement or postyield strain, both indicators of toughness (Table 4). In contrast, postyield energy and total energy increased due to ZOL, with its simultaneous effect of increased ultimate force and yield force appearing to be the driver for more area under the curve (Figure 10). The contrast of whole bone and tissue level results is interesting and suggests that on the tissue level, ZOL did not have an effect on the organic matrix, but did influence bone geometry and mineral on the whole bone level. Examining the tibia, Stadelmann, Bonnet, and Pioletti (2011) conducted a study in 17 week old C57BL/6 male mice, with a single dose of ZOL (100 μg/kg). Compared to age-matched VEH animals, ZOL produced significant increases in stiffness, ultimate force, and postyield energy of 31%, 24%, and 60%, respectively, 11 days after administration. Although the dose of ZOL was high, the direction of these results is in agreement with the current study, with ZOL conferring mechanical elastic effects in a mouse of similar age, genetics, and gender.

In a study using a dose of 100 μg/kg in adult rats, Smith and Allen (2013)

found that 5 weeks postinjection, ZOL had no significant effect on postyield energy, total energy, or other measures of bone plasticity, consistent with the results of the current study. Interestingly, the authors did find that the rate of application of force during the 3-pt bending test altered results of toughness. Compared to VEH, ZOL only reduced plasticity and toughness measurements when the test was conducted at the slower rate of loading (0.03 mm/s) compared to the faster rate of loading (0.3 mm/s). Their results support the rate of force application selected for the current study, which was a relatively similar slower rate (0.01 mm/s). Further work should be conducted to investigate the contribution of the rate of force application in tests with plasticity outcomes. Differences in the dose of ZOL dose (100 μg/kg vs 45 μg/kg in the current study) and drug latency periods (5 weeks vs 3 weeks in the current study) may contribute to the finding of no decrease in bone toughness in the current study.

Other drug studies have examined energy absorption and toughness. Using ibandronate or risendronate, Shahnazari et al. (2010) found that monthly injections of these bisphosphonates for 4 months resulted in no significant change of fracture toughness in aged and ovariectomized (sham-ovariectomized, ± bisphosphonate), control rats, consistent with the current study's results. It should be noted that femoral toughness was measured from nano-indentation tests, rather than the 3-pt bend used in the current study. While using a different drug type and ovariectomized rats, Shahnazari et al. (2010) did present evidence that longer-term bisphosphonate treatment in adult rats

resulted in no alterations of femoral fracture toughness.

Other studies using the 3-pt bending method have found effects of bisphosphonate treatment on the plasticity of rodent bone. Gasser et al. (2008) performed a ZOL study lasting 8 months, using ovariectomized rats that had a starting age of 7 months. The authors presented evidence that toughness, in terms of total energy, was only increased by ZOL at considerably higher doses (100 and 500 μg/kg). These results are in agreement with the current study's finding that ZOL did not increase ductility, measured by postyield displacement. Additionally, the authors found significant bone stiffness increases compared to ovariectomized rats. The Gasser et al. (2008) study is a noteworthy comparison, suggesting that the behavior of bone plasticity and toughness may be temporally dependent, with an additional key factor being tissue age. In contrast to the concept of Currey (2012), these data from Gasser et al. (2008) suggest that a substantial increase in stiffness does not necessarily equate to reductions in toughness.

After 10 months of twice weekly administrations of alendronate (28 μg/kg) in ovariectomized rats, Ma and colleagues (2003) reported through 3-pt bending that toughness, in terms of total energy, was significantly higher compared to baseline and sham controls. These results are consistent with the current study, and opposite to the concept described by Currey (2012). Drawing meaningful comparisons with the Ma et al. (2003) study is limited due to differences such as bisphosphonate type, dosage, duration of treatment, measurement technique,

and animal model. Luo and Allen (2013) found reduced rib toughness and a normal rate of remodeling in mature, female dogs after 9 months of biweekly ZOL injections (60 μg/kg). With an increase in stiffness and a decrease in postyield displacement, their work is in agreement with the concept proposed by Currey (2012). The animals were not in a state of imposed bone loss, such as simulated weightlessness or postmenopausal. The older age of the animals (1 to 2 years of age) is worthy to note, with cortical bone naturally having a greater mean tissue age because of its slower turnover rate. A slower turnover in cortical bone would result in less new, less mineralized, and more ductile bone. It seems warranted to consider that the lifespan of bone toughness may undulate according to bone selection, subject age, and treatment. While the Luo & Allen (2013) study is noteworthy since zoledronate and toughness were investigated, important limitations to consider are that the bone mechanically tested was not weight-bearing, and the frequency of ZOL injections far exceeded normal clinical dosages.

Combined Treatment Effects

The combined treatment results of the current study showed that the ZOL-treated mice experiencing simulated weightlessness increased femoral stiffness, preventing the deleterious effects of HU. The HU mice treated with ZOL did not concurrently present with diminished plasticity, rejecting the principal hypothesis of this study. Interestingly, for postyield displacement, the combined treatment effects were additive, with ZOL not modulating the HU effect. Zoledronate

conferred benefits to the bone, allowing greater forces to be incurred prior to a yielding of the bone and permanent deformation. The combined treatment conclusions for mechanical properties are shown in Figure 11.

In terms of structure, the combined treatment results showed that the ZOL-treated mice experiencing simulated weightlessness increased their cortical thickness, preventing HU losses. In the combined treatment of ZOL+HU, cancellous bone volume fraction trended highly (interaction, $p = 0.17$), as did trabecular number (interaction, $p = 0.07$), with the raw data showing a substantial difference in the ZOL-treated animals. These data suggest that ZOL was able to maintain cortical thickness during 3 weeks of HU, and subtly confer a trending protective effect for cancellous parameters. These structural data help substantiate the increase of stiffness in the mechanical properties.

Limitations

One limitation of this study is the need for a larger sample size to increase statistical power, especially for cancellous HU losses. Another limitation is the 3 week duration for ZOL to act upon the bones of the mice. Longer term ZOL treatment studies should be conducted to understand its effect on mechanical properties in the context of astronauts performing 2-3 year missions to Mars. Additionally, future studies should investigate the effectiveness of ZOL in countering bone loss and bone quality decrements. The dog rib has been examined during long duration bisphosphonate treatment (alendronate, risedronate) and has shown consistent reductions in bone toughness over 1 to 3

years (Allen & Burr, 2011; Allen, Reinwald, & Burr, 2008; Mashiba et al., 2000). These studies show that bisphosphonates reduce the amount of energy the bone can absorb before fracturing, but not in subjects experiencing bone losses from unloading or estrogen deficiency. In order to draw conclusions for the structural and mechanical health of bone in astronauts, such study designs and treatments should be considered. For human subjects, bed rest disuse studies have also been an analog to mimic spaceflight effects on bone and should be considered to understand the efficacy of countermeasures such as ZOL (LeBlanc, Spector, Evans, & Sibonga, 2007).

Notwithstanding, several studies are worthy of scientific comparison because they show that the effect of a bisphosphonate in reducing toughness has a temporal dependence and often only presents after longer duration treatments. Compelling work by Burr, Liu, and Allen (2015) provided evidence that during the first year of alendronate treatment (0.2 mg/kg, once a day) there was, in fact, a trending increase in bone toughness. Beyond 1 year, the authors found reduced bone toughness until the end of the 3-year study. Future studies should examine the effect of long duration ZOL treatment on mechanical properties of bone.

In human subjects, researchers found that 3 years after a single intravenous dose of ZOL, biomarkers of bone remodeling remained significantly suppressed compared to baseline (Grey et al., 2010). Along with other bisphosphonates, ZOL is under consideration for use by astronauts during long-

term spaceflight missions. Future space travel has the prospect of lasting 3 years or more. With this is mind, LeBlanc and colleagues (2013) investigated the efficacy of alendronate and exercise in mitigating bone loss in astronauts after an average 5.5 months of spaceflight aboard the ISS. With exercise in space being an essential routine, all subjects taking the antiresorptive treatment exercised as well. The combined treatment of alendronate and exercise was effective in counteracting predictable declines in bone physiological parameters associated with spaceflight.

The amount of time ZOL has to act on bone is worth consideration, as is the age of the subject. Ng and collaborators (2015) presented a compelling model to investigate the condition of adynamic bone. This condition is relatively common in chronic kidney disease, a condition where both bone formation and bone resorption are reduced, leading to thin osteoids, decreased osteoblasts and osteoclasts, and reductions in bone toughness. This condition has also been suspected to result from long duration antiresorptive treatments, such as bisphosphonates. The authors found that reductions in bone toughness were more severe in older mice (16 months old) who were induced into presenting with this adynamic condition compared to younger mice (4 months old). The investigators also made an interesting point that while bone toughness in the older mice was severely degraded compared to young, their bone mineral density and structural data were normal. This indicates that the other bony constituents, not measured with μCT, contributed to the reductions of toughness,

namely bone collagen and associated organic components.

Additionally, comparing 4 month old and 16 month old controls, Ng et al. (2015) found reductions in toughness and postyield displacement only in the axially compressed vertebrae (L3, L4), and not in the 3-pt bending femur mechanical results. With mouse vertebrae containing a substantial percentage of cancellous tissue, this suggests the preferential role of cancellous tissue in toughness changes, which was not captured in their femoral 3-pt bending tests. Moreover, comparing the 4 month old and 16 month old controls, substantial reductions in mineral apposition rates showed that osteoblasts were less active in older mice, and consequently responsible for the decrease of cancellous bone and toughness. This provides strong cellular evidence that aged tissue in the cancellous compartment of the mouse vertebrae is disproportionately underpinning toughness changes. In future studies, the selection of bone and the age of the subject are important variables to consider when examining effects on bone toughness.

The current study found that HU resulted in statistically significant decreases in bodyweight of the mice compared to NA controls (-10%, p = 0.0001). Amblard et al. (2003) found that after 2 weeks of tail suspension, C57BL/6 male 4 month old mice weighed significantly less than ambulatory controls. Lloyd, Loiselle, Zhang, and Donahue (2014) found that after 3 weeks of HU of both wild-type mice and connexin 43-deficient knockout mice (male, 6 months old), bodyweight losses were significant at -5% and -3%, respectively,

compared to their genetic controls. This is in contrast to Alwood et al. (2010) who reported no significant differences in body mass after 2 weeks of HU of 4 month old C57BL/6 male mice. Earlier research on the effect of HU on bodyweight and stress biomarkers primarily used the rat model (Halloran, Bikle, Cone, & Morey-Holton, 1988; Morey-Holton & Globus, 2002). Results from the current study and contrasting evidence in the literature points to the need for close monitoring of bodyweight and possible use of ANCOVA for statistical analysis.

Bone Stiffness and Plasticity

A central limitation in this study was no direct measurement of collagen. Bone is a composite material of both inorganic and organic components. Collagen is critical, in that the organic matrix plays an integral role in the toughness of bone and its plasticity. Mineral is disproportionately responsible for stiffness and strength (ultimate force), but the behavior of bone once yield and permanent deformation occur is largely due to collagen (Allen & Burr, 2007; Burr, 2002; Wang, Shen, Li, & Agrawal, 2002). As permanent deformation occurs at yield, the bone will no longer be able to return to its original shape. It is primarily the collagen and the organic matrix still withstanding the load, playing a crucial role in the resulting ductility or brittleness. Brittleness can be defined as the lessening of the postyield or plastic region. This brittleness manifests both in terms of postyield displacement as well as the magnitude of strain, or point of displacement upon the yielding of the bone (Burr, 2002). This study likely altered

the mineral-to-matrix ratio in the cancellous bone with ZOL, along with the treatments (HU, ZOL) influencing measurements of geometry and amount of bone. The mechanical 3-pt bending test resulted in a fracture of the entire bone, enabling measurements of postyield displacement and forces, stresses, and strains within that region. Conclusions were drawn based on the contrasting results between the whole bone and tissue level measurements. However, without a direct collagen measurement, a critical component for a comprehensive analysis and cause of bone plasticity behavior is lacking. Conclusions regarding whether HU or ZOL impacted collagen cross-linking or the stability of helical collagen fibrils cannot be drawn (Viguet-Carrin et al., 2006).

To elucidate the role of other bone compartments in mechanical and material properties, other techniques may be employed. Such methods include procedures to reveal cellularity, and dynamic indices to examine bone remodeling rates and bone microdamage. Fluorescence measurement techniques can measure collagen with its crosslinks, and vibrational spectroscopy techniques, which excite chemical bonds in minerals and proteins, are being further developed to measure microscale and nanoscale outcomes (Donnelly, 2011).

Based upon mineral being stiffer than bone collagen, Currey (2012) suggested there is trade off, so that if a bone becomes very stiff, there will be a corresponding reduction in toughness. This concept doesn't consider several important factors that contribute to bone mechanical properties. Based upon

data from this study and the literature review, it appears that bone undergoes undulating lifespan changes in mechanical properties corresponding with osteoblast and osteoclast changes that impact the bone collagen matrix, mineral, and structure (Burr et al., 2015; Kuroshima et al. 2012; Ng et al., 2015). Additionally, the lifespan changes seem to be site-specific, depending on the composition of the bony compartment. These age-related cellular and site-specific changes should be considered in the Currey thesis, as they may have a significant impact on bone remodeling quality (stiffness vs. toughness) by inhibiting efforts to repair bone microdamage, resulting in greater fracture risk.

Further Work and Conclusions

Further research is warranted to assess the risks to skeletal health in long term space travel. The basic science precedes the translational science, with the hope that work with animals and ground analogs will help to inform decisions for astronaut health regimens. Future studies should consider a model that specifically modulates toughness, in conjunction with mitigation regimens to elucidate not only the elastic, but also the plasticity behavior of bone in microgravity. Additional research should also examine possible risks to skeletal health when long-term resistance training, antiresorptive drugs, and microgravity are combined. Chronic suppression of normal bone remodeling, paired with aged bone that is undergoing repeated loading of the skeleton with exercise, may lead to accumulated, unrepaired microdamage and, perhaps, stress fractures.

Although collagen was not directly measured, certain conclusions are merited due to the measurement of plasticity, stiffness, and geometry. Zoledronate maintained bone structure and increased stiffness during simulated weightlessness, while not reducing postyield displacement. Zoledronate was effective in preventing bone losses of structure and stiffness, similar to what astronauts might lose from microgravity. At the same time, brittleness did not occur. Further studies are warranted, but based upon the current data, use of zoledronate as a countermeasure to bone loss could help safeguard astronaut skeletal health during future space missions.

References

Akhter, M. P., Iwaniec, U. T., Covey, M. A., Cullen, D. M., Kimmel, D. B., & Recker, R. R. (2000). Genetic variations in bone density, histomorphometry, and strength in mice. *Calcified Tissue International*, *67*, 337-344. doi:10.1007/s002230001144

Akhter, M. P., Fan, Z., & Rho, J. Y. (2004). Bone intrinsic material properties in three inbred mouse strains. *Calcified Tissue International*, *75*, 416-420. doi:10.1007/s00223-004-0241-7

Allen, M. R., & Burr, D. B. (2007). Mineralization, microdamage, and matrix: How bisphosphonates influence material properties of bone. *BoneKEy-Osteovision*, *4*, 49-60. doi:10.1138/20060248

Allen, M. R., & Burr, D. B. (2011). Bisphosphonate effects on bone turnover, microdamage, and mechanical properties: What we think we know and what we know that we don't know. *Bone*, *49*, 56-65. doi:10.1016/j.bone.2010.10.159

Allen, M. R., Reinwald, S., & Burr, D. B. (2008). Alendronate reduces bone toughness of ribs without significantly increasing microdamage accumulation in dogs following 3 years of daily treatment. *Calcified Tissue International, 82*, 354-360. doi:10.1007/s00223-008-9131-8

Alwood, J. S., Yumoto, K., Mojarrab, R., Limoli, C. L., Almeida, E. A. C., Searby, N. D., & Globus, R. K. (2010). Heavy ion irradiation and unloading effects on mouse lumbar vertebral microarchitecture, mechanical properties and tissue stresses. *Bone*, *47*, 248-255. doi:10.1016/j.bone.2010.05.004

Amblard, D., Lafage-Proust, M. H., Laib, A., Thomas, T., Rüegsegger, P., Alexandre, C., & Vico, L. (2003). Tail suspension induces bone loss in skeletally mature mice in the C57BL/6J strain but not in the C3H/HeJ strain. *Journal of Bone and Mineral Research*, *18*, 561-569. doi:10.1359/jbmr.2003.18.3.561

Amin, D., Cornell, S. A., Gustafson, S. K., Needle, S. J., Ullrich, J. W., Bilder, G. E., & Perrone, M. H. (1992). Bisphosphonates used for the treatment of bone disorders inhibit squalene synthase and cholesterol biosynthesis. *Journal of Lipid Research*, *33*, 1657-1663. Retrieved from http://www.jlr.org/content/33/11/1657.short

Beaupre, G. S., Orr, T. E., & Carter, D. R. (1990). An approach for time-dependent bone modeling and remodeling--theoretical development. *Journal of Orthopedic Research, 8*, 651-661. doi:10.1002/jor.1100080506

Blaber, E. A., Dvorochkin, N., Torres, M. L., Yousuf, R., Burns., B. P., Globus, R. K., & Almeida, E. A. C. (2014). Mechanical unloading of bone in microgravity reduces mesenchymal and hematopoietic stem cell-mediated tissue regeneration. *Stem Cell Research, 13*, 181-201. doi:10.1016/j.scr.2014.05.005

Boivin, G. Y., Chavassieux, P. M., Santora, A. C., Yates, J., & Meunier, P. J. (2000). Alendronate increases bone strength by increasing the mean degree of mineralization of bone tissue in osteoporotic women. *Bone*, *27*, 687-694. doi:10.1016/S8756-3282(00)00376-8

Bonadio, J., Jepsen, K. J., Mansoura, M. K., Jaenisch, R., Kuhn, J. L., & Goldstein, S. A. (1993). A murine skeletal adaptation that significantly increases cortical bone mechanical properties. Implications for human skeletal fragility. *Journal of Clinical Investigation*, *92*, 1697-1705. doi:10.1172/JCI116756

Bonewald, L. F. (2011). The amazing osteocyte. *Journal of Bone and Mineral Research*, *26*, 229-238. doi:10.1002/jbmr.320

Bouxsein, M. L., Boyd, S. K., Christiansen, B. A., Guldberg, R. E., Jepsen, K. J., & Müller, R. (2010). Guidelines for assessment of bone microstructure in rodents using micro-computed tomography. *Journal of Bone and Mineral Research, 25*, 1468-1486. doi:10.1002/jbmr.141

Boyle, W. J., Simonet, W. S., & Lacey, D. L. (2003). Osteoclast differentiation and activation. *Nature*, *423*(6937), 337-342. doi:10.1038/nature01658

Brodt, M. D., Ellis, C. B., & Silva, M. J. (1999). Growing C57Bl/6 mice increase whole bone mechanical properties by increasing geometric and material properties. *Journal of Bone and Mineral Research*, *14*, 2159-2166. doi:10.1359/jbmr.1999.14.12.2159

Burr, D. B. (2002). The contribution of the organic matrix to bone's material properties. *Bone*, *31*, 8-11. doi:10.1016/S8756-3282(02)00815-3

Burr, D. B., Miller, L., Grynpas, M., Li, J., Boyde, A., Mashiba, T., … Johnston, C. C. (2003). Tissue mineralization is increased following 1-year treatment with high doses of bisphosphonates in dogs. *Bone*, *33*, 960-969. doi:10.1016/j.bone.2003.08.004

Burr, D. B., Liu, Z., & Allen, M. R. (2015). Duration-dependent effects of clinically relevant oral alendronate doses on cortical bone toughness in beagle dogs. *Bone*, *71*, 58-62. doi:10.1016/j.bone.2014.10.010

Calliot-Augusseau, A., Lafage-Proust, M., Soler, C., Pernod, J., Dubois, F., & Alexandre, C. (1998). Bone formation and resorption biological markers in cosmonauts during and after a 180-day space flight (Euromir 95). *Clinical Chemistry, 44,* 578-585. Retrieved from http://www.clinchem.org/content/44/3/578.full

Chambers, T. J., & Magnus, C. J. (1982). Calcitonin alters behaviour of isolated osteoclasts. *The Journal of Pathology*, *136*, 27-39. doi:10.1002/path.1711360104

Collet, P., Uebelhart, D., Vico, L., Moro, L., Hartmann, D., Roth, M., & Alexandre, C. (1997). Effects of 1- and 6-month spaceflight on bone mass and biochemistry in two humans. *Bone, 20*, 547-551. doi:10.1016/S8756-3282(97)00052-5

Coxon, F. P., & Taylor, A. (2008). Vesicular trafficking in osteoclasts. *Seminars in Cell & Developmental Biology, 19*, 424-433. doi:10.1016/j.semcdb.2008.08.004

Coxon, F. P., Thompson, K., & Rogers, M. J. (2006). Recent advances in understanding the mechanism of action of bisphosphonates. *Current Opinions in Pharmacology, 6*, 307-312. doi:10.1016/j.coph.2006.03.005

Crockett, J. C., Rogers, M. J., Coxon, F. P., Hocking, L. J., & Helfrich, M. H. (2011). Bone remodelling at a glance. *Journal of Cell Science*, *124*, 991-998. doi:10.1242/jcs.063032

Currey, J. (2012). The structure and mechanics of bone. *Journal of Material Science, 47*, 41-54. doi:10.1007/s10853-011-5914-9

Currey, J. D., Brear, K., & Zioupos, P. (1996). The effects of ageing and changes in mineral content in degrading the toughness of human femora. *Journal of Biomechanics*, *29*, 257-260. doi:10.1016/0021-9290(95)00048-8

Doblaré, M., GarcÍa, J. M., & Gómez, M. J. (2004). Modelling bone tissue fracture and healing: A review. *Engineering Fracture Mechanics*, *71*, 1809-1840. doi:10.1016/j.engfracmech.2003.08.003

Donnelly, E. (2011). Methods for assessing bone quality: A review. *Clinical Orthopaedics and Related Research*, 469, 2128-2138. doi:10.1007/s11999-010-1702-0

Dunford, J. E., Thompson, K., Coxon, F. P., Luckman, S. P., Hahn, F. M., Poulter, C. D., ... Rogers, M. J. (2001). Structure-activity relationships for inhibition of farnesyl diphosphate synthase in vitro and inhibition of bone resorption in vivo by nitrogen-containing bisphosphonates. *Journal of Pharmacology and Experimental Therapeutics*, *296*, 235-242. Retrieved from http://jpet.aspetjournals.org/content/296/2/235.short

Ebetino, F. H., Hogan, A. M. L., Sun, S., Tsoumpra, M. K., Duan, X., Triffitt, J. T., … Russell, R. G. G. (2011). The relationship between the chemistry and biological activity of the bisphosphonates. *Bone*, *49*, 20-33. doi:10.1016/j.bone.2011.03.774

Ferguson, V. L., Ayers, R. A., Bateman, T. A., & Simske, S. J. (2003). Bone development and age-related bone loss in male C57BL/6J mice. *Bone, 33*, 387-398. doi:10.1016/S8756-3282(03)00199-6

Ferretti, J. L., Capozza, R. F., Mondelo, N., & Zanchetta, J. R. (1993). Interrelationships between densitometric, geometric, and mechanical properties of rat femora: Inferences concerning mechanical regulation of bone modeling. *Journal of Bone and Mineral Research*, *8*, 1389-1396. doi:10.1002/jbmr.5650081113

Flurkey, K., Currer, J. M., & Harrison, D. E. (2007). Mouse models in aging research. In: J. G. Fox et al. (Eds.), *The mouse in biomedical research* (2nd ed., Vol. 3, pp. 637–672). Burlington, MA: Elsevier Academic Press. Retrieved from http://mouseion.jax.org/stfb2000_2009/1685

Franz-Odendaal, T. A., Hall, B. K., & Witten, P. E. (2006). Buried alive: How osteoblasts become osteocytes. *Developmental Dynamics*, *235*, 176-190. doi:10.1002/dvdy.20603

Fratzl, P., & Weinkamer, R. (2007). Nature's hierarchical materials. *Progress in Materials Science*, *52*, 1263-1334. doi:10.1016/j.pmatsci.2007.06.001

Frost, H. M. (2003). Bone's mechanostat: A 2003 update. *The Anatomical Record Part A: Discoveries in Molecular, Cellular, and Evolutionary Biology*, *275,* 1081-1101. doi:10.1002/ar.a.10119

Fyhrie, D. P., & Christiansen, B. A. (2015). Bone material properties and skeletal fragility. *Calcified Tissue International*, *97*, 213-228. doi:10.1007/s00223-015-9997-1

Gasser, J. A., Ingold, P., Venturiere, A., Shen, V., & Green, J. R. (2008). Long-term protective effects of zoledronic acid on cancellous and cortical bone in the ovariectomized rat. *Journal of Bone and Mineral Research*, *23*, 544-551. doi:10.1359/JBMR.071207

Gere, J. M., & Timoshenko, S. (1984). *Mechanics of materials.* Boston: PWS-Kent.

Globus, R. K., & Morey-Holton, E. (2016). Hindlimb unloading: Rodent analog for microgravity. *Journal of Applied Physiology*, *120,* 1196-1206. doi:10.1152/japplphysiol.00997.2015

Granke, M., Does, M. D., & Nyman, J. S. (2015). The role of water compartments in the material properties of cortical bone. *Calcified Tissue International*, *97*, 292-307. doi:10.1007/s00223-015-9977-5

Grey, A., Bolland, M., Wattie, D., Horne, A., Gamble, G., & Reid, I. R. (2010). Prolonged antiresorptive activity of zoledronate: A randomized, controlled trial. *Journal of Bone and Mineral Research*, *25*, 2251-2255. doi:10.1002/jbmr.103

Halloran, B. P., Bikle, D. D., Cone, C. M., & Morey-Holton, E. (1988). Glucocorticoids and inhibition of bone formation induced by skeletal unloading. *American Journal of Physiology-Endocrinology and Metabolism, 255*, E875-E879. Retrieved from http://ajpendo.physiology.org/content/255/6/E875

Halloran, B. P., Ferguson, V. L., Simske, S. J., Burghardt, A., Venton, L. L., & Majumdar, S. (2002). Changes in bone structure and mass with advancing age in the male C57BL/6J mouse. *Journal of Bone and Mineral Research, 17*, 1044-1050. doi:10.1359/jbmr.2002.17.6.1044

Hamrick, M. W., McPherron, A. C., Lovejoy, C. O., & Hudson, J. (2000). Femoral morphology and cross-sectional geometry of adult myostatin-deficient mice. *Bone*, *27*, 343-349. doi:10.1016/S8756-3282(00)00339-2

Heer, M. A., Baecker, N., Mika, C., Boese, A., & Gerzer, R. (2005). Immobilization induces a very rapid increase in osteoclast activity. *Acta Astronautica, 57*, 31-36. doi:10.1016/j.actaastro.2004.12.007

Iwaniec, U. T., Wronski, T. J., Amblard, D., Nishimura, Y., van der Meulen, M. C. H., Wade, C. E., ... Globus, R. K. (2005). Effects of disrupted β1-integrin function on the skeletal response to short-term hindlimb unloading in mice. *Journal of Applied Physiology*, *98*, 690-696. doi:10.1152/japplphysiol.00689.2004

Iwata, K., Mashiba, T., Hitora, T., Yamagami, Y., & Yamamoto, T. (2014). A large amount of microdamages in the cortical bone around fracture site in a patient of atypical femoral fracture after long-term bisphosphonate therapy. *Bone*, *64*, 183-186. doi:10.1016/j.bone.2014.04.012

Jämsä, T., Jalovaara, P., Peng, Z., Väänänen, H. K., & Tuukkanen, J. (1998). Comparison of three-point bending test and peripheral quantitative computed tomography analysis in the evaluation of the strength of mouse femur and tibia. *Bone*, *23*, 155-161. doi:10.1016/S8756-3282(98)00076-3

Jepsen, K. J., Pennington, D. E., Lee, Y. L., Warman, M., & Nadeau, J. (2001). Bone brittleness varies with genetic background in A/J and C57BL/6J inbred mice. *Journal of Bone and Mineral Research*, *16*, 1854-1862. doi:10.1359/jbmr.2001.16.10.1854

Jepsen, K. J., Silva, M. J., Vashishth, D., Guo, X. E., & van der Meulen, M. C. H. (2015). Establishing biomechanical mechanisms in mouse models: Practical guidelines for systematically evaluating phenotypic changes in the diaphyses of long bones. *Journal of Bone and Mineral Research*, *30*, 951-966. doi:10.1002/jbmr.2539

Jing, D., Cai, J., Wu, Y., Shen, G., Li, F., Xu, Q., ... Wu, X. (2014). Pulsed electromagnetic fields partially preserve bone mass, microarchitecture, and strength by promoting bone formation in hindlimb-suspended rats. *Journal of Bone and Mineral Research*, *29*, 2250-2261. doi:10.1002/jbmr.2260

Judex, S., Garman, R., Squire, M., Busa, B., Donahue, L. R., & Rubin, C. (2004). Genetically linked site specificity of disuse osteoporosis. *Journal of Bone and Mineral Research*, *19*, 607-613. doi:10.1359/JBMR.040110

Kavanagh, K. L., Guo, K., Dunford, J. E., Wu, X., Knapp, S., Ebetino, F. H., … Oppermann, U. (2006). The molecular mechanism of nitrogen-containing bisphosphonates as antiosteoporosis drugs. *Proceedings of the National Academy of Sciences*, *103*, 7829-7834. doi:10.1073/pnas.0601643103

Ke, H. Z., Shen, V. W., Qi, H., Crawford, D. T., Wu, D. D., Liang, X. G., … Thompson, D. D. (1998). Prostaglandin E2 increases bone strength in intact rats and in ovariectomized rats with established osteopenia. *Bone*, *23*, 249-255. doi:10.1016/S8756-3282(98)00102-1

Kerschnitzki, M., Wagermaier, W., Roschger, P., Seto, J., Shahar, R., Duda, G. N., … Fratzl, P. (2011). The organization of the osteocyte network mirrors the extracellular matrix orientation in bone. *Journal of Structural Biology*, *173*, 303-311. doi:10.1016/j.jsb.2010.11.014

Keyak, J. H., Koyama, A., K., LeBlanc, A., Lu, Y., & Lang, T. F. (2009). Reduction in proximal femoral strength due to long-duration spaceflight. *Bone, 44*, 449-453. doi:10.1016/j.bone.2008.11.014

Khajuria, D. K., Razdan, R., & Mahapatra, D. R. (2015). Effect of combined treatment with zoledronic acid and propranolol on mechanical strength in an rat model of disuse osteoporosis. *Revista Brasileira de Reumatologia (English Edition)*, *55*, 501-511. doi:10.1016/j.rbre.2014.07.007

Kodama, Y., Umemura, Y., Nagasawa, S., Beamer, W. G., Donahue, L. R., Rosen, C. R., … Farley, J. R. (2000). Exercise and mechanical loading increase periosteal bone formation and whole bone strength in C57BL/6J mice but not in C3H/Hej mice. *Calcified Tissue International*, *66*, 298-306. doi:10.1007/s002230010060

Kuroshima, S., Go, V. A. A., & Yamashita, J. (2012). Increased numbers of nonattached osteoclasts after long-term zoledronic acid therapy in mice. *Endocrinology*, *153*, 17-28. doi:10.1210/en.2011-1439

Lakkakorpi, P. T., & Väänänen, H. K. (1996). Cytoskeletal changes in osteoclasts during the resorption cycle. *Microscopy Research and Technique*, *33,* 171-181. doi:10.1002/(SICI)1097-0029(19960201)33:2<171::AID-JEMT7>3.0.CO;2-W

Lang, T., LeBlanc, A., Evans, H., Lu, Y., Genant, H., & Yu, A. (2004). Cortical and trabecular bone mineral loss from the spine and hip in long-duration spaceflight. *Journal of Bone and Mineral Research, 19,* 1006-1012. doi:10.1359/JBMR.040307

LeBlanc, A., Lin, C., Shackelford, L., Sinitsyn, V., Evans, H., Belichenko, O., … Feeback, D. (2000). Muscle volume, MRI relaxation times (T2), and body composition after spaceflight. *Journal of Applied Physiology, 89*, 2158-2164. Retrieved from http://jap.physiology.org/content/89/6/2158.short

LeBlanc, A., Matsumoto, T., Jones, J., Shapiro, J., Lang, T., Shackelford, L., … Ohshima, H. (2013). Bisphosphonates as a supplement to exercise to protect bone during long-duration spaceflight. *Osteoporosis International, 24*, 2105-2114. doi:10.1007/s00198-012-2243-z

LeBlanc, A. D., Spector, E. R., Evans, H. J., & Sibonga, J. D. (2007). Skeletal responses to space flight and the bed rest analog: A review. *Journal of Musculoskeletal and Neuronal Interactions*, *7*, 33-47. Retrieved from http://www.ismni.org/jmni/pdf/27/07LEBLANC.pdf

Lloyd, S. A., Loiselle, A. E., Zhang, Y., & Donahue, H. J. (2014). Evidence for the role of connexin 43-mediated intercellular communication in the process of intracortical bone resorption via osteocytic osteolysis. *BMC Musculoskeletal Disorders*, *15*, 1-8. doi:10.1186/1471-2474-15-122

Lloyd, S. A., Travis, N. D., Lu, T., & Bateman, T. A. (2008). Development of a low-dose anti-resorptive drug regimen reveals synergistic suppression of bone formation when coupled with disuse. *Journal of Applied Physiology*, *104*, 729-738. doi:10.1152/japplphysiol.00632.2007

Loehr, J. A., Lee, S. M. C., English, K. L., Sibonga, J., Smith, S. M., Spiering, B. A., & Hagan, R. D. (2010). Musculoskeletal adaptations to training with the advanced resistive exercise device. *Medicine & Science in Sports & Exercise, 43,* 146-156. doi:10.1249/MSS.0b013e3181e4f161

Luo, T. D., & Allen, M. R. (2013). Short-courses of dexamethasone abolish bisphosphonate-induced reductions in bone toughness. *Bone*, *56*, 199-203. doi.org/10.1016/j.bone.2013.06.004

Luxenburg, C., Geblinger, D., Klein, E., Anderson, K., Hanein, D., Geiger, B., & Addadi, L. (2007). The architecture of the adhesive apparatus of cultured osteoclasts: From podosome formation to sealing zone assembly. *PLoS ONE*, *2,* e179. doi:10.1371/journal.pone.0000179

Luxenburg, C., Parsons, J. T., Addadi, L., & Geiger, B. (2006). Involvement of the Src-cortactin pathway in podosome formation and turnover during polarization of cultured osteoclasts. *Journal of Cell Science*, *119*, 4878-4888. doi:10.1242/jcs.03271

Ma, Y. L., Bryant, H. U., Zeng, Q., Schmidt, A., Hoover, J., Cole, H. W., ... Sato, M. (2003). New bone formation with teriparatide [human parathyroid hormone-(1–34)] is not retarded by long-term pretreatment with alendronate, estrogen, or raloxifene in ovariectomized rats. *Endocrinology*, *144*, 2008-2015. doi:10.1210/en.2002-221061

Manolagas, S. C. (2000). Birth and death of bone cells: Basic regulatory mechanisms and implications for the pathogenesis and treatment of osteoporosis 1. *Endocrine Reviews*, *21*, 115-137. doi:10.1210/edrv.21.2.0395

Mashiba, T., Hirano, T., Turner, C. H., Forwood, M. R., Johnston, C. C., & Burr, D. B. (2000). Suppressed bone turnover by bisphosphonates increases microdamage accumulation and reduces some biomechanical properties in dog rib. *Journal of Bone and Mineral Research*, 15, 613-620. doi:10.1359/jbmr.2000.15.4.613

Mellis, D. J., Itzstein, C., Helfrich, M. H., & Crockett, J. C. (2011). The skeleton: A multi-functional complex organ. The role of key signalling pathways in osteoclast differentiation and in bone resorption. *Journal of Endocrinology*, *211*, 131-143. doi:10.1530/JOE-11-0212

Morey-Holton, E. R., & Globus, R. K. (1998). Hindlimb unloading of growing rats: A model for predicting skeletal changes during space flight. *Bone*, *22*, 83-88. doi:10.1016/S8756-3282(98)00019-2

Morey-Holton, E. R., & Globus, R. K. (2002). Hindlimb unloading rodent model: Technical aspects. *Journal of Applied Physiology, 92*, 1367-1377. doi:10.1152/japplphysiol.00969.2001

Nabavi, N., Khandani, A., Camirand, A., & Harrison, R. E. (2011). Effects of microgravity on osteoclast bone resorption and osteoblast cytoskeletal organization and adhesion. *Bone, 49*, 965-974. doi:10.1016/j.bone.2011.07.036

Nancollas, G. H., Tang, R., Phipps, R. J., Henneman, Z., Gulde, S., Wu, W., … Ebetino, F. H. (2006). Novel insights into actions of bisphosphonates on bone: Differences in interactions with hydroxyapatite. *Bone*, *38*, 617-627. doi:10.1016/j.bone.2005.05.003

National Research Council (US) Committee for the Update of the Guide for the Care and Use of Laboratory Animals (2011). *Guide for the Care and Use of Laboratory Animals* [8th ed.]. Washington (DC): National Academies Press. Retrieved from http://www.ncbi.nlm.nih.gov/books/NBK54050/ doi: 10.17226/12910

Neve, A., Corrado, A., & Cantatore, F. P. (2011). Osteoblast physiology in normal and pathological conditions. *Cell and Tissue Research*, *343*, 289-302. doi:10.1007/s00441-010-1086-1

Ng, A. H., Omelon, S., Variola, F., Allo, B., Willett, T. L., Alman, B. A., & Grynpas, M. D. (2015). Adynamic bone decreases bone toughness during aging by affecting mineral and matrix. *Journal of Bone and Mineral Research*, *31*, 369-379. doi:10.1002/jbmr.2702

Orriss, I. R., Burnstock, G., & Arnett, T. R. (2010). Purinergic signalling and bone remodelling. *Current Opinion in Pharmacology*, *10*, 322-330. doi:10.1016/j.coph.2010.01.003

Orwoll, E. S., Adler, R. A., Amin, S., Binkley, N., Lewiecki, E. M., Petak, S. M., … Sibonga, J. D., (2013). Skeletal health in long-duration astronauts: Nature, assessment, and management recommendations from the NASA Bone Summit. *Journal of Bone and Mineral Research*, *28*, 1243-1255. doi:10.1002/jbmr.1948

Ory, S., Brazier, H., Pawlak, G., & Blangy, A. (2008). Rho GTPases in osteoclasts: Orchestrators of podosome arrangement. *European Journal of Cell Biology*, *87*, 469-477. doi:10.1016/j.ejcb.2008.03.002

Plotkin, L. I., Bivi, N., & Bellido, T. (2011). A bisphosphonate that does not affect osteoclasts prevents osteoblast and osteocyte apoptosis and the loss of bone strength induced by glucocorticoids in mice. *Bone*, *49*, 122-127. doi:10.1016/j.bone.2010.08.011

Pozzi, S., Vallet, S., Mukherjee, S., Cirstea, D., Vaghela, N., Santo, L., … Schoonmaker, J. (2009). High-dose zoledronic acid impacts bone remodeling with effects on osteoblastic lineage and bone mechanical properties. *Clinical Cancer Research*, *15*, 5829-5839. doi:10.1158/1078-0432.CCR-09-0426

Reid, I. R (2009). Osteonecrosis of the jaw — Who gets it, and why? *Bone, 44,* 4-10. doi:10.1016/j.bone.2008.09.012

Reid, I. R*.,* Brown, J. P., Burckhardt, P., Horowitz, Z., Richardson, P., Trechsel, U., … Meunier, P. J. (2002). Intravenous zoledronic acid in postmenopausal women with low bone mineral density. *New England Journal of Medicine, 346*, 653-661. doi:10.1056/NEJMoa011807

Rogers, M. J., Gordon, S., Benford, H. L., Coxon, F. P., Luckman, S. P., Monkkonen, J., & Frith, J. C. (2000). Cellular and molecular mechanisms of action of bisphosphonates. *Cancer*, *88*(S12), 2961-2978. doi: 10.1002/1097-0142(20000615)88:12+<2961::AID-CNCR12>3.0.CO;2-L

Russell, R. G. G. (2011). Bisphosphonates: The first 40 years. *Bone*, *49*, 2-19. doi:10.1016/j.bone.2011.04.022

Schriefer, J. L., Robling, A. G., Warden, S. J., Fournier, A. J., Mason, J. J., & Turner, C. H. (2005). A comparison of mechanical properties derived from multiple skeletal sites in mice. *Journal of Biomechanics, 38*, 467-475. doi:10.1016/j.jbiomech.2004.04.020

Shahnazari, M., Kurimoto, P., Boudignon, B. M., Orwoll, B. E., Bikle, D. D., & Halloran, B. P. (2012). Simulated spaceflight produces a rapid and sustained loss of osteoprogenitors and an acute but transitory rise of osteoclast precursors in two genetic strains of mice. *American Journal of Physiology-Endocrinology and Metabolism*, *303*, E1354-E1362. doi:10.1152/ajpendo.00330.2012

Shahnazari, M., Yao, W., Dai, W., Wang, B., Ionova-Martin, S. S., Ritchie, R. O., ... Lane, N. E. (2010). Higher doses of bisphosphonates further improve bone mass, architecture, and strength but not the tissue material properties in aged rats. *Bone*, *46*, 1267-1274. doi:10.1016/j.bone. 2009.11.019

Shane, E., Burr, D., Ebeling, P. R., Abrahamsen, B., Adler, R. A., Brown, T. D., ... Dempster, D. (2010). Atypical subtrochanteric and diaphyseal femoral fractures: Report of a task force of the American Society for Bone and Mineral Research. *Journal of Bone and Mineral Research*, *25*, 2267-2294. doi:10.1002/jbmr.253

Shirazi-Fard, Y., Kupke, J. S., Bloomfield, S. A., & Hogan, H. A. (2013). Discordant recovery of bone mass and mechanical properties during prolonged recovery from disuse. *Bone*, *52*, 433-443. doi:10.1016/ j.bone.2012.09.021

Silva, M. J., Brodt, M. D., Wopenka, B., Thomopoulos, S., Williams, D., Wassen, M. H., … Bank, R. A. (2006). Decreased collagen organization and content are associated with reduced strength of demineralized and intact bone in the SAMP6 mouse. *Journal of Bone and Mineral Research*, *21*, 78-88. doi:10.1359/JBMR.050909

Silverman, S., & Christiansen, C. (2012). Individualizing osteoporosis therapy. *Osteoporosis International*, *23*, 797-809. doi:10.1007/s00198-011-1775-y

Smith, E. A., Frankenburg, E. P., Goldstein, S. A., Koshizuka, K., Elstner, E., Said, J., … Koeffler, H. P. (2000). Effects of long-term administration of vitamin D3 analogs to mice. *Journal of Endocrinology*, *165*, 163-172. doi:10.1677/joe.0.1650163

Smith, E. R., & Allen, M. R. (2013). Bisphosphonate-induced reductions in rat femoral bone energy absorption and toughness are testing rate-dependent. *Journal of Orthopaedic Research*, *31*, 1317-1322. doi:10.1002/jor.22343

Smith, S. M., Abrams, S. A., Davis-Street, J., Heer, M. A., O'Brien, K., Wastney, M., & Zwart, S. (2014). Fifty years of human space travel: Implications for bone and calcium research. *Annual Review of Nutrition, 34*, 377-400. doi:10.1146/annurev-nutr-071813-105440

Smith, S. M., Heer, M. A., Shackelford, L. C., Sibonga, J. D., Ploutz-Snyder, L., & Zwart, S. R. (2012). Benefits for bone from resistance exercise and nutrition in long-duration spaceflight: Evidence from biochemistry and densitometry. *Journal of Bone and Mineral Research, 27*, 1896-1906. doi:10.1002/jbmr.1647

Smith, S. M., Wastney, M. E., O'Brien, K. O., Morukov, B., V., Larina, I. M., Abrams, S. … Shackelford, L. C. (2005). Bone markers, calcium metabolism, and calcium kinetics during extended-duration space flight on the Mir Space Station. *Journal of Bone and Mineral Research, 20*, 208-218. doi:10.1359/JBMR.041105

Smith, S. M., Zwart, S. R., Block, G., Rice, B. L., & Davis-Street, J. E. (2005). The nutritional status of astronauts is altered after long-term space flight aboard the International Space Station. *Journal of Nutrition, 135*, 437-443. Retrieved from http://jn.nutrition.org/content/135/3/437.long

Spatz, J. M., Ellman, R., Cloutier, A. M., Louis, L., van Vliet, M., Suva, L. J., … Bouxsein, M. L. (2013). Sclerostin antibody inhibits skeletal deterioration due to reduced mechanical loading. *Journal of Bone and Mineral Research*, *28*, 865-874. doi:10.1002/jbmr.1807

Stadelmann, V. A., Bonnet, N., & Pioletti, D. P. (2011). Combined effects of zoledronate and mechanical stimulation on bone adaptation in an axially loaded mouse tibia. *Clinical Biomechanics*, *26*, 101-105. doi:10.1016/j.clinbiomech.2010.08.014

Stenbeck, G., Lawrence, K. M., & Albert, A. P. (2012). Hormone-stimulated modulation of endocytic trafficking in osteoclasts. *Frontiers in Endocrinology*, *3*(103), 1-9. doi:10.3389/fendo.2012.00103

Tamma, R., Colaianni, G., Camerino, C., Di Benedetto A., Greco G., Strippoli, M., … Zallone, A. (2009). Microgravity during spaceflight directly affects in vitro osteoclastogenesis and bone resorption. *FASEB Journal, 23*, 2549-2554. doi:10.1096/fj.08-127951

Turner, C. H., & Burr, D. B. (1993). Basic biomechanical measurements of bone: A tutorial. *Bone, 14*, 595-608. doi:10.1016/8756-3282(93)90081-K

Turner, C. H., Hsieh, Y. F., Müller, R., Bouxsein, M. L., Baylink, D. J., Rosen, C. J., … Beamer, W. G. (2000). Genetic regulation of cortical and trabecular bone strength and microstructure in inbred strains of mice. *Journal of Bone and Mineral Research*, *15*, 1126-1131. doi:10.1359/jbmr.2000.15.6.1126

Turner, R. T. (2000). Invited review: What do we know about the effects of spaceflight on bone? *Journal of Applied Physiology*, *89*, 840-847. Retrieved from http://jap.physiology.org/content/89/2/840

van der Meulen, M. C. H., & Boskey, A. L. (2012). Atypical subtrochanteric femoral shaft fractures: Role for mechanics and bone quality. *Arthritis Research & Therapy*, *14*, 1-8. doi:10.1186/ar4013

Vico, L., Collet, P., Guignandon, A., Lafage-Proust, M. H., Thomas, T., Rehailia, M., & Alexandre, C. (2000). Effects of long-term microgravity exposure on cancellous and cortical weight-bearing bones of cosmonauts. *Lancet, 355*, 1607-1611. doi:10.1016/S0140-6736(00)02217-0

Viguet-Carrin, S., Garnero, P., & Delmas, P. D. (2006). The role of collagen in bone strength. *Osteoporosis International*, *17*, 319-336. doi:10.1007/s00198-005-2035-9

Voide, R., van Lenthe, G. H., & Müller, R. (2008). Bone morphometry strongly predicts cortical bone stiffness and strength, but not toughness, in inbred mouse models of high and low bone mass. *Journal of Bone and Mineral Research*, *23*, 1194-1203. doi:10.1359/JBMR.080311

Wagermaier, W., Klaushofer, K., & Fratzl, P. (2015). Fragility of bone material controlled by internal interfaces. *Calcified Tissue International*, *97*, 201-212. doi:10.1007/s00223-015-9978-4

Wang, X., Shen, X., Li, X., & Agrawal, C. M. (2002). Age-related changes in the collagen network and toughness of bone. *Bone*, *31*, 1-7. doi:10.1016/S8756-3282(01)00697-4

Weivoda, M. M., & Oursler, M. J. (2014). The roles of small GTPases in osteoclast biology. *Orthopedic & Muscular System: Current Research*, *3,* 161-168. doi:10.4172/2161-0533.1000161

Wergedal, J. E., Sheng, M. C., Ackert-Bicknell, C. L., Beamer, W. G., & Baylink, D. J. (2002). Mouse genetic model for bone strength and size phenotypes: NZB/B1NJ and RF/J inbred strains. *Bone*, *31*, 670-674. doi:10.1016/S8756-3282(02)00908-0

Wergedal, J. E., Sheng, M. H. C., Ackert-Bicknell, C. L., Beamer, W. G., & Baylink, D. J. (2005). Genetic variation in femur extrinsic strength in 29 different inbred strains of mice is dependent on variations in femur cross-sectional geometry and bone density. *Bone*, *36*, 111-122. doi:10.1016/j.bone.2004.09.012

Zaidi, M., Inzerillo, A. M., Moonga, B. S., Bevis, P. J. R., & Huang, C. H. (2002). Forty years of calcitonin—where are we now? A tribute to the work of Iain Macintyre, FRS. *Bone*, *30*, 655-663. doi:10.1016/S8756-3282(02)00688-9

Zhang, F. L., & Casey, P. J. (1996). Protein prenylation: Molecular mechanisms and functional consequences. *Annual Review of Biochemistry*, *65*, 241-269. doi:10.1146/annurev.bi.65.070196.001325

Zioupos, P., Currey, J. D., & Hamer, A. J. (1999). The role of collagen in the declining mechanical properties of aging human cortical bone. *Journal of Biomedical Materials Research*, *45*, 108-116. doi:10.1002/(SICI)1097-4636(199905)45:2<108::AID-JBM5>3.0.CO;2-A